HYDROLOGICAL PROCESSES
Hydrol. Process. (2012)
Published online in Wiley Online Library
(wileyonlinelibrary.com) DOI: 10.1002/hyp.9283

Modelling spatial and temporal variability of hydrologic impacts of climate change in the Fraser River basin, British Columbia, Canada

Rajesh R. Shrestha,* Markus A. Schnorbus, Arelia T. Werner and Anne J. Berland

Pacific Climate Impacts Consortium, University House 1, PO Box 3060 Stn CSC, University of Victoria, Victoria, BC, Canada, V8W 3R4

Abstract:

This paper presents a modelling study on the spatial and temporal variability of climate-induced hydrologic changes in the Fraser River basin, British Columbia, Canada. This large basin presents a unique modelling case due to its physiographic heterogeneity and the potentially large implications of changes to its hydrologic regime. The macro-scale Variable Infiltration Capacity (VIC) hydrologic model was employed to simulate 30-year baseline (1970s) and future (2050s) hydrologic regimes based on climate forcings derived from eight global climate models (GCMs) runs under three emissions scenarios (B1, A1B and A2). Bias Corrected Spatial Disaggregation was used to statistically downscale GCM outputs to the resolution of the VIC model (1/16°). The modelled future scenarios for the 11 sub-basins and three regions (eastern mountains, central plateau and coastal mountains) of the FRB exhibit spatially varied responses, such as, shifts from snow-dominant to hybrid regime in the eastern and coastal mountains and hybrid to rain-dominant regime in the central plateau region. The analysis of temporal changes illustrated considerable uncertainties in the projections obtained from an ensemble of GCMs and emission scenarios. However, direction of changes obtained from the GCM ensembles and emissions scenarios are consistent amongst one another. The most significant temporal changes could include earlier onsets of snowmelt-driven peak discharge, increased winter and spring runoff and decreased summer runoff. The projected winter runoff increases and summer decreases are more pronounced in the central plateau region. The results also revealed increases in the total annual discharge and decreases in the 30-year mean of the peak annual discharge. Such climate-induced changes could have implications for water resources management in the region. The spatially and temporally varied hydro-climatic projections and their range of projections can be used for local-scale adaptation in this important water resource system for British Columbia. Copyright © 2012 John Wiley & Sons, Ltd.

KEY WORDS climate change; Fraser River basin; hydrologic impacts; snow hydrology; VIC model

Received 11 August 2011; Accepted 21 February 2012

INTRODUCTION

The hydrologic regime of the Fraser River basin (FRB), British Columbia, Canada is dominated by snow accumulation and melt processes. Snow normally accumulates throughout the winter except in lower elevation areas of the basin and annual peak flow predominantly occurs during snowmelt in spring or early summer (Moore and Wondzell, 2005). The winter discharge of such basins is typically low, while in summer, the discharge declines rapidly following the depletion of the snow storage. The snowmelt-driven discharge plays an important role in the region's water supply. For instance, one of the FRB headwater tributaries, the Nechako River is regulated for hydroelectric generation with water storage during the spring snowmelt period and releases during the remainder of the year (Mundie and Bell-Irving, 1986). Snowmelt is also a major flood producing mechanism in many watersheds in the region (Whitfield *et al*. 2003; Cunderlik and Ouarda, 2009).

Climate change is generally expected to lead to an intensification of the global water cycle (Huntington, 2006), which is likely to influence freshwater quantity and quality with respect to both mean states and variability (Kundzewicz *et al*., 2007). The volume, extent and seasonality of snowpack, and the associated snowmelt runoff for snow-dominated mountain regions are intrinsically linked to climate variability and change (Stewart, 2009). Changes in precipitation principally affect maximum snow accumulation and runoff volume while temperature changes mostly affect runoff timing (Barnett *et al*., 2005). In the Pacific North-West (PNW) region, where the FRB is located (Moore and Wondzell, 2005), impacts of changing climate to the snow hydrology is already evident, such as reductions in the snow water contents and earlier snowmelt and discharge (e.g. Mote *et al*., 2005; Stewart *et al*., 2005; Adam *et al*., 2009; Stewart, 2009). Recent detection and attribution studies of hydrologic changes in the western United States also found evidence of human-induced changes to hydrology and snowpack between 1950 and 1999 (Barnett *et al*., 2008), and observed trends toward earlier timing of snowmelt-driven discharges since 1950 are detectably different from natural variability (Hidalgo *et al*., 2009). Furthermore,

*Correspondence to: Rajesh R. Shrestha, Pacific Climate Impacts Consortium, University House 1, PO Box 3060 Stn CSC, University of Victoria, Victoria, BC, Canada V8W 3R4.
E-mail: rshresth@uvic.ca

by isolating only the warm Pacific Decadal Oscillation periods, Hamlet *et al.* (2005) found downward trends in April 1st snow water equivalent (SWE) over the western United States to be primarily due to widespread warming, which are not well explained by decadal climate variability. Such changes in the snow and hydrologic regime are projected to continue in the future by a number of modelling studies (e.g. Merritt *et al.*, 2006; Rauscher *et al.*, 2008; Elsner *et al.*, 2010; Vano *et al.*, 2010). The alterations of the hydrological cycle in snowmelt-dominated regions and consequently loss of natural storage by snowpack could have major implications, such as regional water shortages where built storage capacity is inadequate to cope with seasonal shifts in discharge (Barnett *et al.*, 2005).

Previous studies of the FRB indicate similar past trends and projected future responses. Foreman *et al.* (2001) and Morrison *et al.* (2002) analyzed the historical flow data of the Fraser River (Hope station) since 1912 and found an advance in the annual dates at which one-third and one-half of the total annual discharges occurred. Morrison *et al.* (2002) further used the UBC watershed model driven by two global climate models (GCMs), which projected progressively earlier onset of the peak annual flow through 2020s, 2050s and 2080s, increased mean annual flow and decreased annual peak flow over the three periods. Whitfield *et al.* (2002, 2003) also used the UBC watershed model driven by a GCM to project streamflow for the three future periods (2013–2033, 2043–2063 and 2073–2093) in the Georgia Basin, which included sub-basins of the FRB. The results indicated increased winter flows and an increased number (but not magnitude) of flood events in rainfall-driven streams, an increased number of winter flood events and a decreased number of summer snowmelt flood events in hybrid streams, and increasingly earlier onset of spring snowmelt and increased magnitude and duration of summer flood events in snowmelt-driven streams. The recent study by Kerkhoven and Gan (2011) using the MISBA model driven by seven GCMs for the FRB (Hope station) also projected earlier onset of spring snowmelt and decreased monthly annual peak flow for 2020s, 2050s and 2080s. The mean annual flow was projected to change by $\pm 10\%$.

Future hydrologic changes in a basin depend on basin characteristics, and spatial and temporal variability of climatic conditions (i.e. precipitation and temperature) and their changes. In particular, in the PNW, the future hydrologic changes could be highly varied due to the highly heterogeneous physiographic settings, and temperature and precipitation regimes. For example, Chang and Jung (2010) studied spatial and temporal variability of future runoff changes in 218 sub-basins of the Willamette basin in Oregon and found large reductions in projected summer flow in snowmelt-dominated sub-basins, and large increases in projected winter flow in rainfall-dominated sub-basins. Jung and Chang (2011) further analyzed the same basin and found more pronounced winter runoff changes at higher elevations than at low elevations. Elsner *et al.* (2010) studied implications of climate change on the hydrologic regimes of several watersheds in Washington State and found significant changes to the mean monthly hydrograph in the snow and rain-snow dominant watersheds, and minimal changes to the rain-dominant watershed. Similarly, a hydrologic projection study of the Puget Sound basin by Cuo *et al.* (2011) found shifts to mixed snow-rain-dominated hydrographs in presently snow-dominated basins and increases in December-January flow in the rain-dominated basins.

Given the physiographic and climatological variability of the FRB (Moore, 1991), spatially varied hydrologic response from the basin can be expected. Fleming *et al.* (2007) analyzed streamflow sensitivities to the Pacific climate modes in the Georgia Basin-Puget Sound region, including the lower Fraser River, and found spatially heterogeneous seasonal flow responses to the climate variability in the 20th century. Thorne and Woo (2011) also analyzed the effect of climate variability on streamflow response for 1969–2008 and found response signals to climate variability to be strongly influenced by individual sub-basin responses. Given such highly varied responses to the historical climate variability, it is essential to consider the spatial and temporal variability of the future hydrologic response in individual basins to support future water resources management. However, spatial variability of future hydrologic changes is not available in the previous studies of the FRB.

This paper makes a contribution towards an improved understanding of spatial and temporal variability of climate change impacts in the FRB. For a spatially distributed evaluation of hydrologic responses, the macro-scale Variable Infiltration Capacity (VIC) hydrologic model was employed. The VIC model was used to simulate 30-year baseline (1970s) and future (2050s) hydrologic regimes at a 1/16° grid resolution with climate forcings for the future period derived from eight recent (Intergovernmental Panel on Climate Change (IPCC) Fourth Assessment Report (AR4)) GCMs run under three emissions scenarios (B1, A1B and A2). For a spatially distributed representation of the climate variables, the GCM outputs were downscaled using Bias Corrected Spatial Disaggregation (BCSD) method. The spatial variability of potential future changes was considered for 11 sub-basins and three regions of the FRB. Temporal variability was considered for the daily, monthly and seasonal responses.

Study basin

The FRB is the largest basin in the province of British Columbia, Canada with the drainage area of about 230000 km^2 and relief varying from sea level to about 4000 m. (Figure 1). The river has its headwaters in the Rocky mountains (near Jasper, Alberta) and its main stem runs through a length of about 1400 km before discharging

DOI: 10.1002/hyp

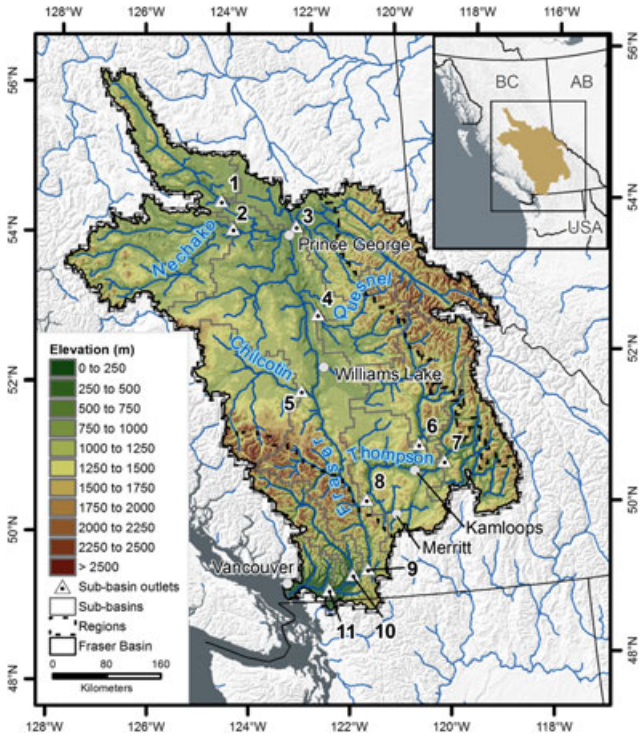

Figure 1. Location map and elevation range of the Fraser River Basin (FRB). The numbers 1–11 are the sub-basins outlets (Table I) corresponding to the Water survey of Canada (WSC) hydrometric stations.

into the Strait of Georgia (Schnorbus *et al.*, 2010). Major tributaries of the Fraser River include the Stuart River, Nechako River, Quesnel River, Chilcotin River, Thompson River and the Harrison River. The FRB is geographically diverse with 12 ecoregions and 9 biogeoclimatic zones (Schnorbus *et al.*, 2010). Land cover in the basin is dominated by coniferous forest (approximately 75% of the basin area), with remaining areas composed of alpine terrain (17%) and various non-forest vegetation (8%) (Schnorbus *et al.*, 2010).

The FRB is home to 63% of BC's population and arguably the economic, social and cultural heartland of British Columbia. Approximately 170 km from the mouth, the river emerges onto lower Fraser valley region, where it flows through braided channels now partially constrained by flood defenses (Rice *et al.*, 2009) with 600 km of dikes (BC Ministry of Environment, http://www.env.gov.bc.ca/wsd/public_safety/flood/brochur2.html#existing). This large floodplain and delta area contains a mix of agricultural, residential and commercial land (approximately $13 billion of development) including Vancouver, Canada's third largest city. Lakes and tributaries within the FRB also provide spawning habitat for all five species of eastern Pacific salmon (Schnorbus *et al.*, 2010), and the basin is a particularly important spawning ground for Sockeye and Chinook salmon, accounting for majority of the Canadian stock (Morrison *et al.*, 2002). Overall, very little consumptive use is made of Fraser River water, with only about 10400 m^3/day licensed to be withdrawn for irrigation from Fraser River and its tributaries (BC Ministry of Environment, http://www.env.gov.bc.ca/wat/wq/objectives/fraserhope/fraserhope.html). Two reservoir systems, the Nechako (890 MW) and Bridge-Seton (492 MW) have been developed in the tributaries of the Fraser River for hydroelectric power generation. However, the main stem of the Fraser River does not consist of storage structures; therefore, capacity to respond to the possible climate-driven changes such as flow volume, flood peak and seasonal shifts in discharge is limited.

Climate variability in the FRB reflects the interaction of the dominant westerly atmospheric circulation with mountain ranges (Moore, 1991). The spatial variability of the mean annual temperature and precipitation for the FRB (based on gridded observations data primarily derived from the Environment Canada climate station observations) is shown in Figure 2. Mean annual temperature and precipitation vary between −5 °C–10 °C and 200 mm–5000 mm, respectively. Except for the low-lying lower Mainland region downstream of the Fraser River at Hope hydrometric station (which receives higher precipitation due to proximity to the coast), the FRB generally receives higher precipitation at higher elevation ranges (Figures 1 and 2b). The hydrologic response of the areas within the FRB can vary considerably, showing snow-dominant, hybrid (rain and snow) or rain dominant response at different parts of the basin (Wade *et al.*, 2001). The mean annual discharge (1965–1990) at the Fraser River at Mission hydrometric station (Water Survey of Canada hydrometric station # 08MH024) is about 3400 m^3/s, with the maximum monthly mean discharge in June (7900 m^3/s) and minimum monthly mean discharge in February (1000 m^3/s). Flow regulation and diversion by the Nechako reservoir delays and reduces the discharge peak

DOI: 10.1002/hyp

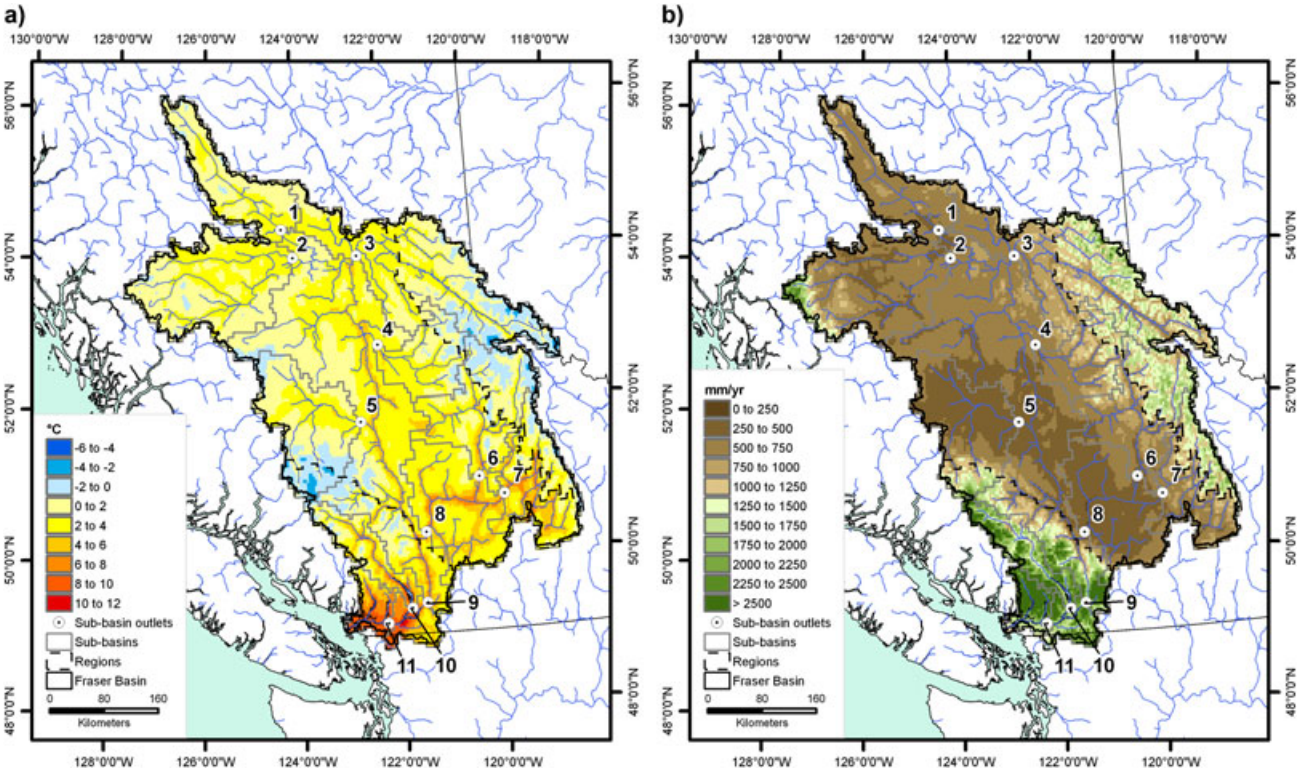

Figure 2. Spatial variability of the 30-year (1961–1990) mean annual a) temperature [°C] and b) precipitation [mm/yr] for the FRB.

in the FRB. The reservoir diverts about 40% of total naturalized discharge out of the FRB at the Nechako River at Vanderhoof hydrometric station (based on 1961–1990 discharge data) via Kemano powerhouse outflow. The effect of flow diversion gets gradually diminished downstream and constitutes about 3.5% and 3% of the total discharge at the Fraser River-Hope and Fraser River-Mission hydrometric stations, respectively. This study does not consider flow regulation but uses the naturalized flow (estimated from the reservoir spillway outflow and powerhouse outflow and adjusted for storage change in the reservoir; obtained from the BC Ministry of Environment, unpublished data) for hydrologic model calibration.

For the consideration of spatially distributed responses, the FRB was divided into 11 sub-basins at the outlets of the major tributaries and the main stem (Figure 1). The sub-basin characteristics are summarized in Table I and the monthly precipitation, temperature and runoff for the period 1961–1990 are compared in Figure 3. The precipitation and temperature data are based on the gridded observations data (mentioned above) and runoff data is based on the water survey of Canada hydrometric station observations. The snowmelt-driven delayed runoff response is apparent in all sub-basins, with runoff increasing as temperature reaches above 0 °C in April. Consequently, despite higher precipitation in autumn and winter, runoff is higher in spring and summer. The precipitation-runoff regimes of the sub-basins also vary considerably. For instance, the Harrison sub-basin receives the highest annual precipitation and generates the highest annual runoff. The sub-basins originating in the eastern rocky mountains (Fraser-Shelly, North Thompson and South Thompson) are relatively wetter compared to the north-eastern sub-basins of Stuart and Nechako, while the Chilcotin sub-basin in the interior region receives the lowest annual precipitation and generates the lowest annual runoff (Table I). The discharge-basin area relations are also similarly varied. While the wettest sub-basin Harrison covers 3.4% of the FRB area and contributes 12.8% of discharge, and the driest sub-basin Chilcotin covers 8.5% of basin area and contributes 3.2% of discharge.

This study further divided the FRB into the three regions: (i) eastern mountains (including rocky and Columbia mountains); (ii) interior Plateau in the central part of basin and (iii) coastal mountains in the south-western part (which also includes parts of lower Fraser valley), following the physiographic settings and hydro-climatic regimes described by Moore (1991). The three regions are characterized by distinct physiographic settings and hydro-climatic conditions, therefore future responses for the three regions could also vary considerably. These three regions were also considered because most of the sub-basins are located within multiple regions and therefore provide mixed signals from the regions. The characteristics of the three regions are summarized in the Table II and mean monthly precipitation, temperature and runoff are illustrated in Figure 4. From the Figure and Table, distinct characteristics can be seen, especially in the precipitation and runoff regimes. Specifically, despite much lower precipitation, December-March runoff is higher in the central plateau compared to eastern mountains, which indicates that some parts of the region generate rainfall-driven runoff. The coastal mountains also generate higher November-March

DOI: 10.1002/hyp

Table I. Water survey of Canada (WSC) hydrometric stations and corresponding study sub-basins characteristics. The sub-basin mean annual precipitation and runoff are for 1961–1990, with runoff obtained by normalizing the hydrometric station discharges by sub-basin areas. Runoff for Nechako, Fraser-Hope and Fraser-Mission sub-basins are based on estimated naturalized discharges

Sub-basin number	Station name	Sub-basin name	WSC ID	Sub-basin area [km^2]	Elevation range [m]			Prec. [mm/yr]	Runoff [mm/yr]
					Min.	Mean	Max.		
1	Stuart River near Fort St. James	Stuart	08JE001	14600	674	1006	2219	661	281
2	Nechako River at Vanderhoof	Nechako	08JC001	25100	383	1060	2740	716	300
3	Fraser River at Shelley	Fraser-Shelly	08 KB001	32400	569	1308	3928	1163	804
4	Quesnel River near Quesnel	Quesnel	08KH006	11500	506	1173	2371	901	660
5	Chilcotin River below Big Creek	Chilcotin	08 MB005	19300	531	1268	2891	490	158
6	North Thompson River at Mclure	North Thompson	08LB064	19600	354	2684	3193	1029	683
7	South Thompson River at Chase	South Thompson	08LE031	16200	338	1228	2883	1038	609
8	Thompson River near Spences Bridge	Thompson-Spences	08LF051	54900	196	1747	3193	844	441
9	Fraser River at Hope	Fraser-Hope	08MF005	217000	29	1330	3928	805	422
10	Harrison River near Harrison Hot Springs	Harrison	08MG013	7680	3	1336	2986	2217	1831
11	Fraser River at Mission	Fraser-Misson	08MH024	228000	0	1321	3928	874	422

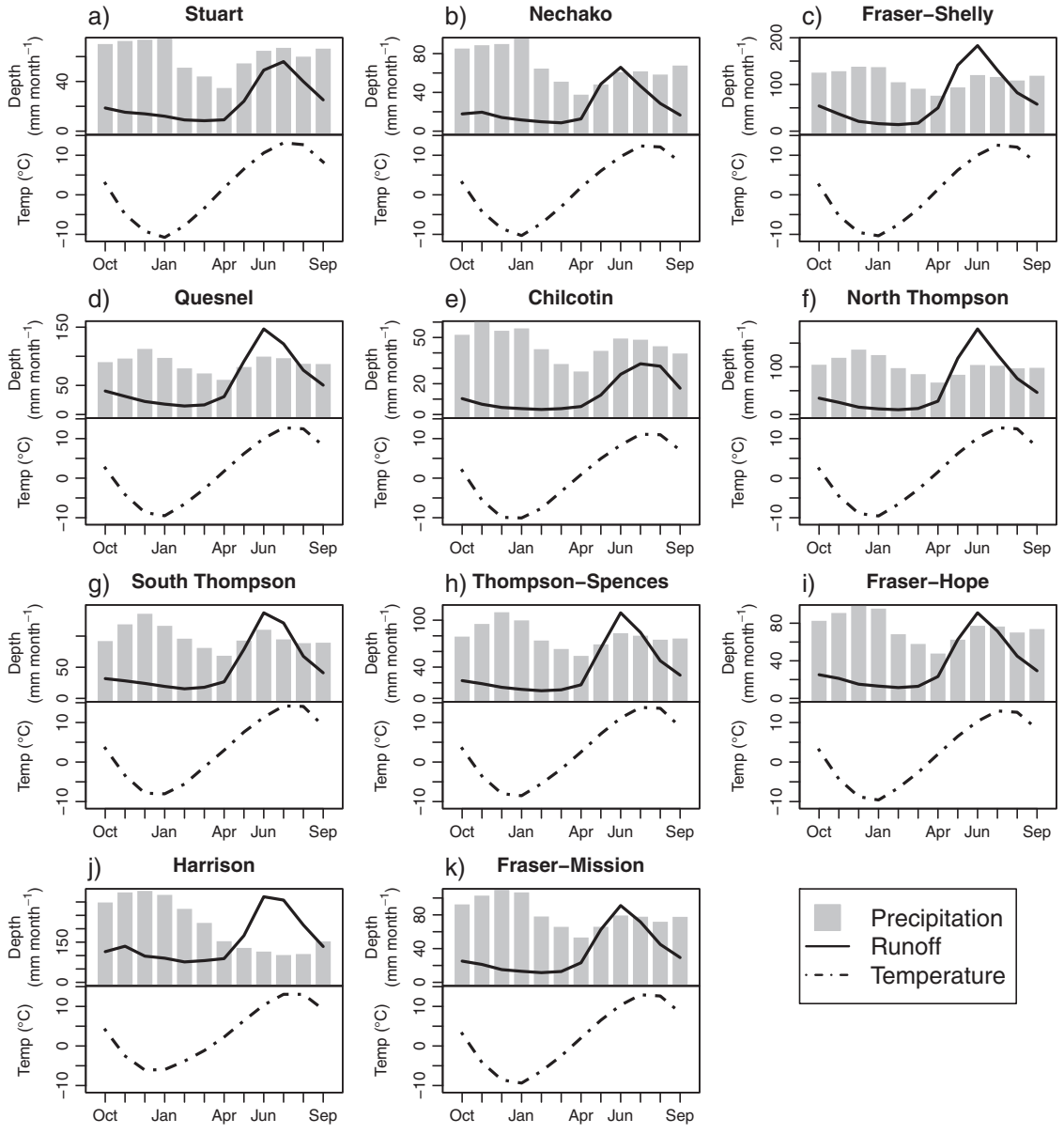

Figure 3. Monthly mean precipitation [mm/month], temperature [°C] and runoff [mm/month] for 11 sub-basins of the FRB, with runoff obtained by normalizing the hydrometric station discharges by sub-basin areas.

DOI: 10.1002/hyp

Table II. Characteristics of the Fraser basin regions. The precipitation and runoff are for 1961–1990, with runoff obtained from VIC model simulated grid cell mean for each region

Region id	Region name	Elevation range [m]			Prec. [mm/yr]	Runoff [mm/yr]
		Min.	Mean	Max.		
I	Eastern mountains	348	1567	3928	1413	1049
II	Interior Plateau	136	1101	3011	621	208
III	Coastal mountains	0	1296	3161	1932	1518

runoff, indicating a rainfall-driven response, especially from the lower Fraser valley. Difference in the hydrologic response amongst the three regions is also illustrated by seasonal runoff ratios (expressed as December-May to June-November ratio). The ratios reveal summer-autumn dominant runoff regimes in the eastern mountains (0.24) and coastal mountains (0.48), and a higher proportion of winter-spring runoff in the central plateau (0.82).

DATA AND METHODS

Climate data

The study used daily gridded observation data for calibration/validation of the hydrologic model and simulation of baseline hydrologic response in the FRB. As described previously, the gridded observation data of maximum and minimum temperature, precipitation and daily average wind speed were derived primarily from the Environment Canada climate station observations, with supplementary inputs from the US Co-operative Station Network, the British Columbia Ministry of Forests and Range's Fire and Weather Network, the British Columbia Ministry of Environment's Automated Snow Pillow network, and BC Hydro's climate network. Precipitation data from Environment Canada's Adjusted Historical Canadian Climate Data (http://ec.gc.ca/dccha-ahccd) was used, which has been corrected for point precipitation biases such as wind undercatch, evaporation and gauge specific wetting losses. Based on these primary data, interpolated gridded data at a spatial resolution of 1/16°, matching the resolution of the hydrologic model was generated. The interpolated data was corrected for elevation effects by adjusting the climatology of the interpolated fields of precipitation and temperature to the 1961–1990 Parameter-Elevation Regressions on Independent Slopes Model (Daly *et al.*, 1994) climatology of the western Canada interpolated to higher resolution using Climate Western North America (ClimateWNA) (Wang *et al.*, 2012). The detailed methodology for the generation of the daily surfaces is described by Maurer *et al.* (2002), and its application over the province of BC is available in Schnorbus *et al.* (2011). Uncertainty in the gridded data arises from low station density at high elevation. Specifically, in the FRB, where 23% of the basin is higher than 1500 m, only 22 out of 420 stations used are located above the 1500 m. As noted by Stahl *et al.* (2006), Rodenhuis *et al.* (2009) and Neilsen *et al.* (2010), the interpolated high-elevation precipitation values are overly influenced by observations from lower elevation sites. Long-term water balance modeling for BC and western North America

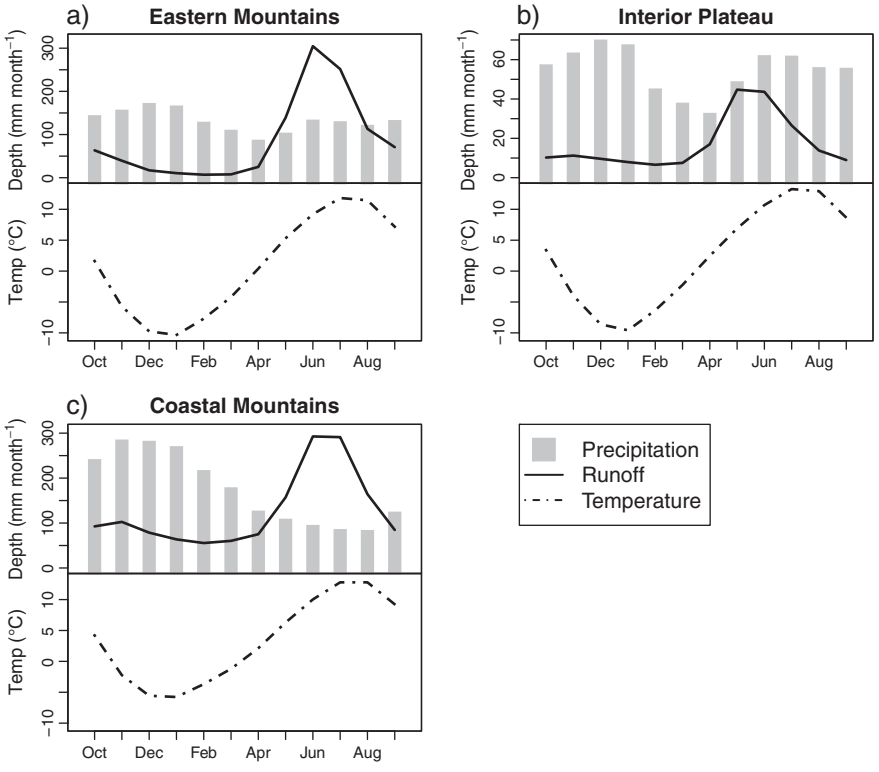

Figure 4. Monthly precipitation [mm/month], temperature [°C] and runoff [mm/month] for three regions of the FRB. Mean runoff is obtained from the average of the VIC model simulated grid runoff for each region.

DOI: 10.1002/hyp

suggests that precipitation bias can typically range between ±40% (Adam *et al*., 2006; Moore *et al*., 2012). In addition, orographic effects could also introduce considerable uncertainty in the gridded precipitation data for the mountainous regions (Adam *et al*., 2006).

An important consideration in the assessment of the future climate impacts is the associated uncertainty (Blöschl and Montanari, 2010). Kay *et al*. (2008) outlined different sources of uncertainties in modelling hydrologic impacts of climate change, which include: future greenhouse gas emissions (forcings); GCM/RCM structure; downscaling method; hydrological model structure; hydrological model parameters and natural variability of the climate system. Previous studies using an ensemble of five GCMs (Kay *et al*., 2008), three GCMs (Prudhomme and Davies, 2008a; 2008b) and eight GCMs (Najafi *et al*., 2011) indicate that GCM structure to be the largest source of uncertainty for the evaluation of hydrologic impacts. Uncertainty associated with the GCMs was also found to be the largest uncertainty source in the recent study of three BC headwater basins (Bennett *et al*., 2012). Therefore, an ensemble of eight IPCC AR4 GCMs was selected based on their historical performance over the globe and more locally over western North America (Werner, 2011). Twenty-three climate change simulations consisting of eight GCMs and three SRES emissions scenarios (A1B, A2 and B1) for each GCM were employed (the UKMO HadGEM1 model does not have output for the B1 scenario), which are summarized in Table III.

The GCM forcings were downscaled to match the resolution of the hydrologic model (1/16°) using the BCSD (Wood *et al*., 2004). BCSD is a statistical downscaling method, which employs relationships between large-scale monthly averages of temperature and precipitation and local-scale temperature and precipitation to develop empirical relationships. The method performs downscaling in three steps: (i) bias correction of the large-scale monthly GCM fields against aggregated gridded observations using quantile mapping (rescaled based on mean and all higher order moments); (ii) spatial disaggregation of the bias-corrected monthly fields to a finer resolution (to match the resolution of the VIC model) using a 'local scaling' approach and (iii) temporal disaggregation of the locally scaled monthly fields corresponding to the daily historic records. BCSD was calibrated to the gridded observations described above for each GCM individually over 1950 to 1999. The downscaled-GCM forcings consisting, of daily precipitation, and minimum and maximum daily temperature, were used as inputs to the hydrologic model for the transient run from 1950 to 2098. Thus, although BCSD explicitly captures the transient nature of a GCMs monthly temperature and precipitation response to an emission scenario, it assumes that future daily variability remains unchanged from historical climatology. Nevertheless, this approach is effective at capturing many aspects of historical daily variability, including temperature extremes, and is competitive in this respect with many other well-known statistical downscaling methods (Maurer and Hidalgo, 2008; Bürger *et al*., 2012). A detailed description of the GCM selection, BCSD and its application for climate projections over BC is available in Werner (2011).

Hydrologic modelling and future climate projections

The macro-scale VIC hydrologic model (Liang *et al*., 1994, 1996) was employed to simulate the hydrologic response in the FRB. The fully spatially distributed VIC model was chosen so that the spatial variability of current and future hydrologic response in the FRB could be evaluated. The spatially distributed representation of the model domain is also suitable for coupling the model with the gridded observation and downscaled GCMs. Suitability of the VIC model for modelling hydrologic response to climate change in similar snowmelt-dominated basins has also been demonstrated extensively by a number of successful applications (e.g. Christensen *et al*., 2004; Christensen and Lettenmaier, 2007; Hidalgo *et al*., 2009; Cherkauer and Sinha, 2010; Schnorbus *et al*., 2011).

VIC is a spatially distributed macro-scale hydrologic model that was originally developed as a soil-vegetation-atmosphere transfer scheme for GCMs. VIC calculates water and energy balances in a grid cell with sub-grid variability of the soil column, land surface vegetation classes and topography represented statistically (Gao *et al*., in review). The model computes the water fluxes for a range of hydrologic processes such as evapotranspiration, snow accumulation, snowmelt, infiltration, soil moisture and surface and subsurface runoffs. The present version of VIC (ver. # 4.07) uses three-soil layers to represent soil moisture processes. The model uses variable infiltration curves to represent the spatial heterogeneity of runoff generation and uses

Table III. GCMs used in this study

GCM	Atmospheric resolution	SRES emissions scenario used	Primary reference
CCSM3	T85 L26	B1, A1B and A2	Collins *et al*. (2006)
CGCM3.1 (T47)	T47 L31	B1, A1B and A2	Scinocca *et al*. (2008)
CSIRO-Mk3.0	T63 L18	B1, A1B and A2	*Rotstayn et al*. (2010)
MPI-OM ECHM5	T63 L32	B1, A1B and A2	Roeckner *et al*. (2006)
GFDL CM2.1	N45 L24	B1, A1B and A2	Delworth *et al*. (2006)
MIROC3.2 (medres)	T42 L20	B1, A1B and A2	K-1 Model Developers (2004)
UKMO-HadCM3	T42 L19	B1, A1B and A2	Collins *et al*. (2001)
UKMO-HadGEM1	N96 L38	A1B and A2	Martin *et al*. (2006)

DOI: 10.1002/hyp

the Arno conceptual model (Todini, 1996) for subsurface flow generation. Surface runoff from the upper two soil layers is generated when the moisture exceeds the storage capacity of the soil. The fluxes from the model are collected and routed downstream using an offline routing routine (Lohmann *et al*., 1998). Detailed description of the VIC model is available in Liang *et al*. (1994, 1996) and Gao *et al*. (in review).

The VIC model was set up for the FRB at 1/16° spatial resolution and daily temporal resolution. Geospatial data for the VIC model were derived from: (i) a 90-m resolution digital elevation model from the NASA Shuttle Radar Topographic Mission (Jarvis *et al*., 2008); (ii) 25-m resolution land cover from the Earth Observation for Sustainable Development of Forests (Wulder *et al*., 2003) upscaled to 1-km resolution and (iii) 1/12° resolution soil classification and parameterization based on Soils Program in the Global Soil Data Products CD-ROM (*Global Soil Data Task*, 2000). The geospatial data were processed and gridded to match the resolution of the VIC model for the entire province of British Columbia (Schnorbus *et al*., 2011).

Forest, the dominant land cover in the FRB, is a dynamic ecosystem wherein the physical components change over time scales of decades to centuries in response to physical, biotic and anthropogenic processes (Kimmins, 2005). It is recognized that climate change will also likely influence future forest cover, and examples include altered wildfire regimes (Marlon *et al*., 2009), species shifts and migrations (Gonzalez *et al*., 2010) and, as emphasized by recent experience in the FRB, changes in pest outbreak severity (Kurz *et al*., 2008). Nevertheless, due to the non-trivial nature of back-casting historical and projecting future transient forest properties, inclusion of the hydrologic effects of dynamic forest cover changes in the hydrologic projections is well beyond the scope of this paper. Consequently, forest cover is assumed static at circa 2000 conditions throughout the projection timeframe.

For a distributed calibration of the VIC model parameters, 61 sub-basins were delineated at Water Survey of Canada hydrometric stations. A set of five parameters and their likely ranges were chosen for the calibration based on the successful calibration of the VIC model in similar snowmelt-dominated basins (Schnorbus *et al*., 2011). The selected parameters include: variable infiltration curve parameter (*Bi*); fraction of maximum soil moisture where non-linear baseflow occurs (*Ws*); maximum velocity of baseflow (*Dsmax*); fraction of *Dsmax* where non-linear baseflow begins (*Ds*); variation of saturated hydraulic conductivity with soil moisture (*Expn*) and maximum velocity of baseflow (*Dsmax*). Demaria *et al*. (2007) found discharge simulation to be most sensitive to *Bi* and *Expn*. Besides these parameters, in view of the uncertainties in the precipitation data, an adjustment factor for precipitation (*Padj*) (which scales the precipitation values within a certain range) was also included for the calibration of runoff in some of the sub-basin.

The VIC model simulated discharges for the sub-basins of the FRB were calibrated using the Multi-Objective Complex evolution Method (Yapo *et al*., 1998). Three objective functions, the Nash–Sutcliffe coefficient of efficiency (NSE), NSE of log-transformed discharge (LNSE) and water balance error (WBE) were considered. The NSE provides a measure of overall 'goodness of fit', with higher values (closer to 1) indicating better agreement, while the LNSE provides a better criterion for the consideration of low flows. The WBE represents the ratio of the difference between cumulative observed and simulated discharges to the cumulative observed discharges, with values closer to zero indicating better agreement. The Pareto solutions from the multi-objective optimization provide trade-offs between the objective functions, which could be employed to diagnose problems in input data and better calibrate the hydrologic model (Shrestha and Rode, 2008). Due to potential problems in the precipitation data, a two-step multi-objective optimization procedure was employed in this study. In the first step, sub-watershed flows were calibrated without precipitation correction. In the second step, in cases when the WBE is $> 20\%$ or $< -20\%$ for the best model performance (according to NSE and LNSE), precipitation data for the sub-catchment were considered unreliable, and the sub-basins was re-calibrated by including the *Padj*. With the inclusion of *Padj* factor in such sub-basins, significant improvement in model performance was observed (not shown). Such sub-basins are also located in the mountainous regions (coastal mountain or eastern mountain regions), where interpolated high-elevation precipitation values are overly influenced by lower elevation stations.

Five independent calibration runs each with an initial population size of 100 and final population size of 25 were performed for each sub-basin. Based on the model performance with respect to the three objective functions from the five calibration runs, the model parameters with the best overall performance were selected by using the fuzzy preference selection methodology (Shrestha and Rode, 2008), which is based on the composite degree of fulfillment of each of the objective functions. Six years (1985–1990) of observed discharge (naturalized discharge for Nechako, Fraser-Hope and Fraser-Mission sub-basins) was used for model calibration and an additional five years (1991–1995) was used for model validation. Calibration was only conducted after a 3-year warm-up period, which was found to be appropriate (by comparing with observations) to exclude the effects of initializing conditions.

The calibrated VIC model for the FRB was forced with daily precipitation, minimum and maximum temperature and wind speed obtained from the 23 BCSD-downscaled GCM runs. The modelled outputs for the 30-year baseline (1970s) and future (2050s) periods were extracted and compared for the 30-year monthly means. The anomalies for the future periods were expressed relative to the 30-year

DOI: 10.1002/hyp

means of the gridded observation-driven baseline run. In addition, magnitude and timing of annual peak discharges were extracted from the daily VIC simulations and averaged over the 30-year baseline and future periods for the comparison of the changes.

RESULTS AND DISCUSSION

VIC calibration results

The validation results for the 11 sub-basins in the FRB are shown in Figure 5, and the statistical performance of the calibration and validation results are summarized in Table IV. Overall, the VIC model is able to reproduce the runoff dynamics for the calibration and validation periods, with the snowmelt peak discharges closely replicated for most years (Figure 5). The statistical performance of the modelled discharge also indicates a good model fit, with NSE and LNSE values greater than 0.70 for most sub-basins. The model performance is generally better for the larger sub-basins such as Thompson-Spences, Fraser-Hope and Fraser-Mission, where, discharges at the upstream sub-basins have been calibrated. The discharge calibration at the upstream sub-basins (which influence the downstream calibration), and size of the basin (local scale 'noise' in the driving meteorological data becomes less important in large sub-basins) are the main factors for better calibration in the larger downstream sub-basins.

There are some discrepancies between the observed and modelled results. Specifically, high negative WBE (i.e. modelled discharge volume is lower than observed discharge volume) were obtained for the Quensel and Chilcotin sub-basins for both calibration and validation periods. The simulated low flow is lower than observations for most sub-basins, and modelled results also show problems in correctly reproducing the secondary peaks, especially in the Harrison sub-basin. The model results also show lower performance for the Nechako sub-basin, which may be due to fact that naturalized discharge was used. The discrepancies in the modelled discharge may also be due in part to problems in the observation dataset, such as produced by river-ice and break-up effects that can lead to major uncertainties in discharge estimates (Pelletier, 1990). In addition, the discrepancies in modelled discharge may also be due to problems in the driving meteorological data, especially at higher elevations where only a few climate stations are located. Further uncertainty in the VIC modelling arises from the model parameters, which are not directly measured and calibrated from observed streamflows. This leads to a problem of equifinality (Beven and Freer, 2001), as many different parameter sets within a chosen model structure can give similar model performance. Issues of model structure, such as lack of accounting of glaciers in the VIC model, also contribute to uncertainties in the hydrologic modelling. Specifically in the FRB, about 1.5 % of the basin is glaciated and the loss of glaciers could significantly impact responses from some of the sub-basins, such as, Harrison (15% glacier coverage), Chilcotin (4.6%), North Thompson (4.3%) and Fraser-Shelly (2.5%). Besides these uncertainties, the discharge simulation of the some of the sub-basins

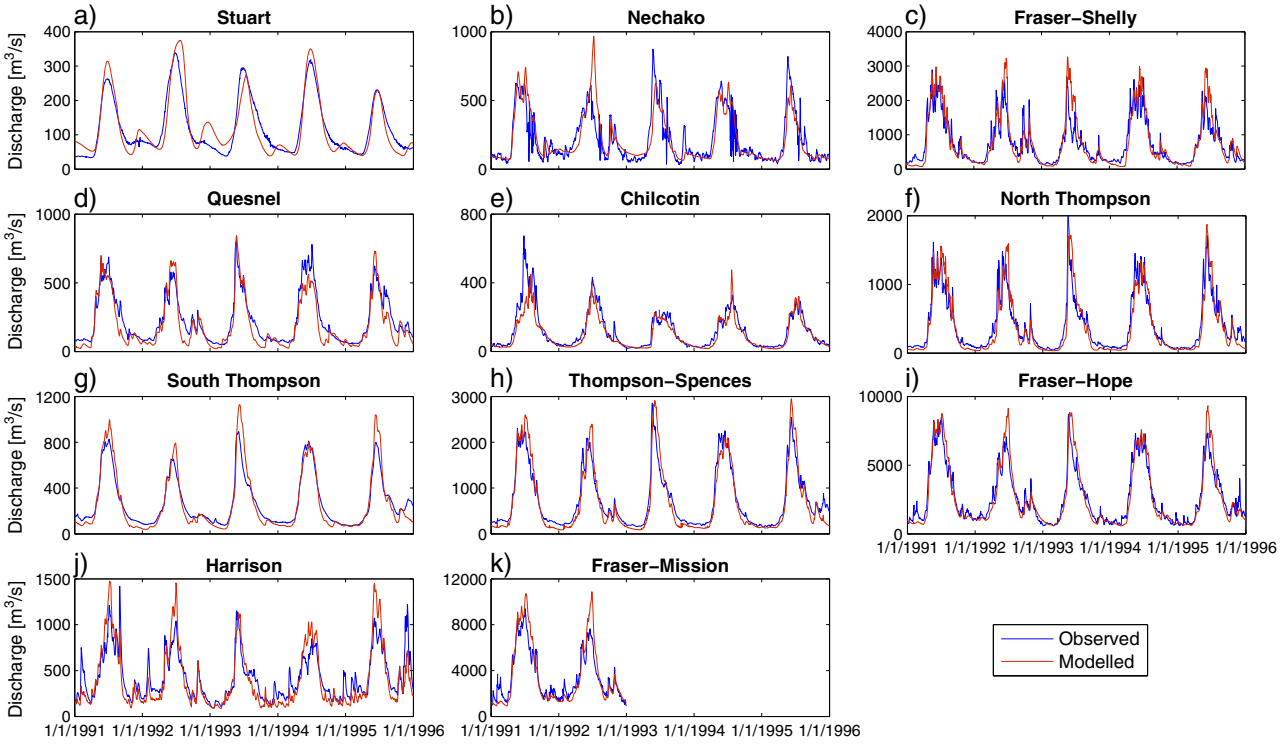

Figure 5. Observed and modelled discharge [m^3/s] for validation results (1991–1995) for the FRB sub-basins. Fraser-Mission is only validated for 1991–1992 because observation data ends in 1992.

DOI: 10.1002/hyp

Table IV. Statistical performance of the VIC calibration (1985–1990) and validation (1991–1995) results for the sub-basins of the FRB. Nash–Sutcliffe coefficient of efficiency (NSE), NSE of log-transformed discharge (LNSE) and water balance error (WBE) were used for the statistical performance. The values in parentheses are for the validation period

Sub-basin number	Sub-basin name	Statistical performance calibration (validation)		
		NSE	LNSE	WBE
1	Stuart	0.84 (0.82)	0.74 (0.71)	−0.01 (0.00)
2	Nechako	0.72 (0.66)	0.71 (0.73)	−0.08 (0.00)
3	Fraser-Shelly	0.85 (0.75)	0.73 (0.70)	−0.05 (0.05)
4	Quesnel	0.88 (0.83)	0.50 (0.52)	−0.16 (−0.16)
5	Chilcotin	0.86 (0.78)	0.89 (0.85)	−0.06 (−0.17)
6	North Thompson	0.87 (0.85)	0.83 (0.77)	−0.04 (−0.07)
7	South Thompson	0.94 (0.87)	0.78 (0.77)	−0.07 (−0.02)
8	Thompson-Spences	0.92 (0.89)	0.84 (0.76)	−0.03 (−0.07)
9	Fraser-Hope	0.91 (0.88)	0.87 (0.89)	−0.02 (−0.01)
10	Harrison	0.79 (0.66)	0.70 (0.61)	−0.02 (−0.06)
11	Fraser-Mission	0.86 (0.79)	0.79 (0.78)	−0.01 (0.03)

such as the Quesnel is also undoubtedly affected by the presence of lakes. Since lakes are not explicitly modelled in the present version of the VIC model, uncertainties associated with estimating evaporation and runoff for the narrow, fjord-type deep lake (mean depth 157 m; Laval *et al.*, 2008) system in the Quesnel sub-basin may contribute to lower LNSE and larger WBE. The lack of inflow and outflow data also precludes direct calibration of the routing model for most lake systems in the FRB, introducing timing errors in routed discharge for sub-basins such as the Quesnel, Stuart, Nechako and South Thompson. The daily time step used for the VIC model run also adds to uncertainties, as the model is unable to account for runoff generation due to sub-daily variations of precipitation such as intense, short-term precipitation events. However, since the model outputs for the baseline and future periods were mainly compared for the 30-year means, uncertainty associated with the daily simulation were not considered to be of a concern. Hence, based on the above validation results, the calibrated VIC hydrologic model was considered suitable to project hydrologic conditions for future climate scenarios.

Temperature and precipitation changes

The BCSD-downscaled median temperature and precipitation outputs from the GCM ensembles are given in Table V. Temperature increases are projected for all seasons and emissions scenarios, with the lowest annual increase for the B1 scenario and the highest annual increase for the A1B scenario in the 2050s. Overall, the median temperature anomalies across the sub-basins and regions of the FRB are similar for each emissions scenario. The inter-GCM variability of the anomalies corresponding to the emissions scenarios are also small annually (range from GCMs, B1: 1.6 °C–1.8 °C; A2:

Table V. Median annual precipitation and temperature anomalies (2050s *versus* 1970s) obtained from the GCM ensembles for the sub-basins and regions of the FRB. The anomalies are given as [°C] change for temperature and [%] change for precipitation

	Temperature anomalies [°C]			Precipitation anomalies [%]		
	B1	A1B	A2	B1	A1B	A2
Sub-basins						
Stuart	1.8	2.5	2.4	12	12	9
Nechako	1.7	2.4	2.3	10	7	5
Fraser-Shelly	1.8	2.5	2.4	10	11	10
Quesnel	1.8	2.6	2.4	7	6	4
Chilcotin	1.8	2.5	2.3	7	3	1
North Thompson	1.8	2.6	2.4	8	8	5
South Thompson	1.8	2.7	2.4	7	6	4
Thompson-Spences	1.8	2.6	2.4	7	6	3
Fraser-Hope	1.8	2.6	2.4	7	6	4
Harrison	1.7	2.6	2.3	7	5	1
Fraser-Mission	1.8	2.6	2.4	6	6	3
Regions						
Eastern mountains	1.7	2.5	2.3	9	10	7
Central Plateau	1.8	2.5	2.3	7	5	3
Coastal mountains	1.7	2.6	2.2	7	3	0

DOI: 10.1002/hyp

2.1 °C–2.4 °C and A1B: 2.4 °C–2.8 °C). Seasonally, greater temperature increase in winter (B1: 1.7 °C–2.5 °C; A2: 2.5 °C–3.2 °C and A1B: 2.5 °C–3.6 °C), and smaller increases in autumn (B1: 1.4 °C–1.8 °C; A2: 2.0 °C–2.4 °C and A1B: 2.3 °C–2.6 °C) are projected (not shown).

Annual precipitation anomalies also show increases for all sub-basins (Table V). Precipitation anomalies amongst the sub-basins show larger variability than temperature with higher increases (for all scenarios) in the northern sub-basins (Stuart, Nechako and Fraser-Hope) compared to the rest of the basin. The magnitude of precipitation increases also vary amongst the three regions, with greater increases in the eastern mountains and lesser increases in the coastal mountains for all three scenarios. Amongst the three emissions scenarios, precipitation increases are generally higher for the B1 scenario. Overall, the mean annual precipitation changes show considerable inter-GCM and inter-regional variability (eastern mountains, B1:3% to 15%; A2: −2% to 15%; A1B 2% to 20%; central plateau: B1:2% to 11%; A2: −5% to 11%; A1B −6% to 18%; and the coastal mountains: B1: −1% to 9%; A2: −7% to 13%; A1B −5% to 18%) (not shown).

Future precipitation projections obtained from the GCMs show wide ranges for three regions (Figure 6). The ranges represented by the box and whisker plots correspond to the uncertainty of the projections of the 30-year means of the GCM ensembles. The ranges are greater for July-January and smaller for March-May. Although monthly precipitation amounts vary amongst the three regions, the direction of changes is similar for most months. Specifically, the median precipitation projections for all three scenarios generally exhibit increases between October and June and decreases between July and August. Since the precipitation regime of the coastal mountains region differs from the other regions, future precipitation changes in this region are somewhat different from the rest of the FRB. In particular, the median projection of future precipitation for the region is close to baseline values for February-June, while the rest of the FRB regions exhibits increases during this period.

Snow storage changes

The potential impacts of climate change (in particular precipitation and temperature change) on snow storage were considered for the VIC simulated April 1st SWE anomalies (relative to the mean of 30-year baseline run) and April 1st SWE to October-March precipitation ratio (SWE/P). The SWE/P values of < 0.1, 0.1–0.5 and 0.5 were used to define the rain-dominant, hybrid (or transient) and snow-dominant (or nival) regimes, respectively, following Elsner *et al*. (2010).

The potential future change in the snow storage is evident in the April 1st SWE anomalies, which project declines for all sub-basins and scenarios (except for the B1 scenario for the Harrison sub-basin) (Table VI). The smaller declines for the B1scenario (compared to A2 and A1B scenarios) are mainly due to lower temperature change and greater precipitation increase (Table V) for the scenario. The SWE anomalies for the sub-basins also show spatial variability. Specifically, the changes are smaller for the higher elevation sub-basins (i.e. Fraser-Shelly and

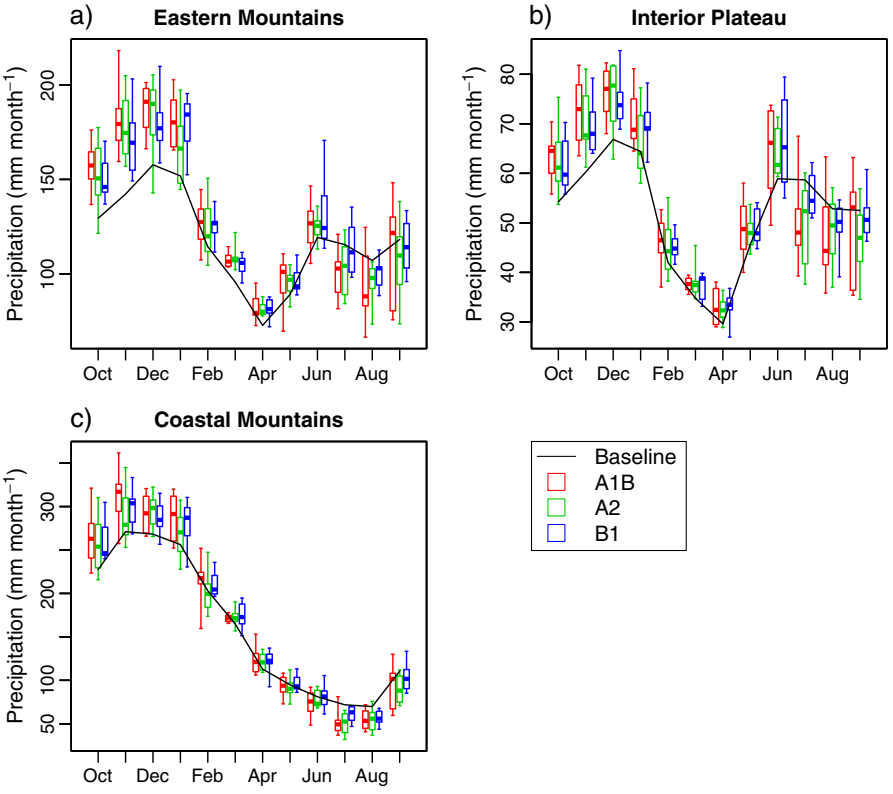

Figure 6. Monthly mean baseline (1970s) and future (2050s) precipitation [mm/month] for the three regions of the FRB. Each box plot illustrates the median and inter-quartile range and the whiskers upper and lower limits from the GCM ensembles.

DOI: 10.1002/hyp

Table VI. GCM ensemble medians of April 1st SWE volume and annual discharge (runoff) changes (2050s *versus* 1970s) for the sub-basins (regions) of the FRB. The SWE and annual runoff change for the regions are for sub-basin grid cell average values. Annual discharge change for the sub-basins is for routed values at the sub-basin outlets

	April 1st SWE change [%]			Flow volume change [%]		
	B1	A1B	A2	B1	A1B	A2
Sub-basins						
Stuart	−30	−41	−38	15	12	7
Nechako	−21	−33	−30	10	8	4
Fraser-Shelly	−6	−15	−17	10	10	7
Quesnel	−19	−31	−31	6	2	0
Chilcotin	−26	−28	−33	9	7	3
North Thompson	−12	−19	−25	9	6	3
South Thompson	−21	−27	−32	10	7	2
Thompson-Spences	−28	−35	−41	9	6	2
Fraser-Hope	−22	−34	−36	7	5	2
Harrison	10	−1	−5	13	11	6
Fraser-Mission	−21	−33	−35	8	6	2
Regions						
Eastern mountains	3	1	−5	9	8	4
Central Plateau	−30	−44	−44	4	0	−4
Coastal mountains	−13	−21	−23	8	6	0

Harrison). Such differences in April 1st SWE signals can also be seen in the comparison of the regional values (Table VI), with the central plateau region showing greater decline and the eastern mountains showing smaller decline. For the coastal mountains region, although higher elevation areas (i.e. Harrison sub-basin, Table VI) show smaller SWE changes, reduced snowfall (due to warmer temperature) in the lower elevations of the Fraser valley leads to an overall decline in snow storage.

The comparison of the median SWE/P thresholds for 1970s with the median of the 2050s GCM ensembles indicates considerable change (Figure 7), with A1B and B1 scenarios showing largest and smallest changes, respectively. The projections for the three scenarios reveal a substantial increase in area with SWE/P < 0.1 and a decrease in area with SWE/P > 0.5, implying increased rain-dominant and decreased snow-dominant areas, respectively. Such changes together with a smaller change in SWE/P = 0.1–0.5 (hybrid regime) indicate a successive transition of parts of the basin from snowfall-dominant to hybrid, and hybrid to rain-dominant regimes. The comparison of the SWE/P values also depicts differences in the future responses in the three regions. In particular, for the snow-dominant eastern and coastal mountains regions, the most prominent changes include the reduction of the areas with SWE/P > 0.5 (range of reduction for the three emissions scenarios; eastern mountains: 16%–21% and coastal mountains: 16%–22%; not shown), indicating a shift from snow-dominant to a hybrid regime. For the central plateau, the most prominent change is the increase in area with SWE/P < 0.1 (14%–21%), indicting a shift from a hybrid to a rain-dominant regime.

Hydrologic changes

The potential future impacts of changes in climatic variables and snow storage can be seen in the evapotranspiration and soil moisture changes (Figure 8). The median A1B (which also represents the greatest change amongst the three emissions scenarios) actual evapotranspiration (AET) increases in spring (Figure 8a), while summer AET is generally characterized by a decline in the central plateau region and an increase in the coastal and eastern mountain regions (Figure 8b). The summer AET decline is simulated despite the increase in potential evapotranspiration (not shown), indicating an increase in soil moisture deficit in the region. Variable regional responses can also be seen for the end of spring (June 1) soil moisture change (Figure 8c). Increased spring AET is accompanied by the end of spring decline in soil moisture in most of the central plateau region, while most of the eastern and coastal mountain regions show increased soil moisture at the end of spring. In addition, although a decline in the end of summer (September 1) soil moisture can be seen throughout the basin, the decline is more pronounced in the coastal and eastern mountains.

Figure 9 depicts the spatial variability of the future runoff changes for the median of A1B ensembles. The results show general increase in the winter and spring runoff and decrease in the summer and autumn runoff. The spatial pattern of change generally reflects the patterns of precipitation, snow storage, AET and soil moisture. For instance, runoff increase (in winter and spring) and decrease (in summer and autumn) for the eastern and coastal mountains regions correspond to the projected precipitation changes in the regions (Figure 6). Spring runoff increases in the eastern and coastal mountains region also correspond to the declines in the snow-dominant area in these regions (Figure 7). Therefore, higher precipitation and earlier snowmelt can be considered to be responsible for the higher spring runoff in the mountain regions. For the summer season, decreased precipitation (Figure 6) and a consequent decline in soil moisture (Figure 8d) lead to a decline in runoff. Decreased October and November precipitation, and increased AET

DOI: 10.1002/hyp

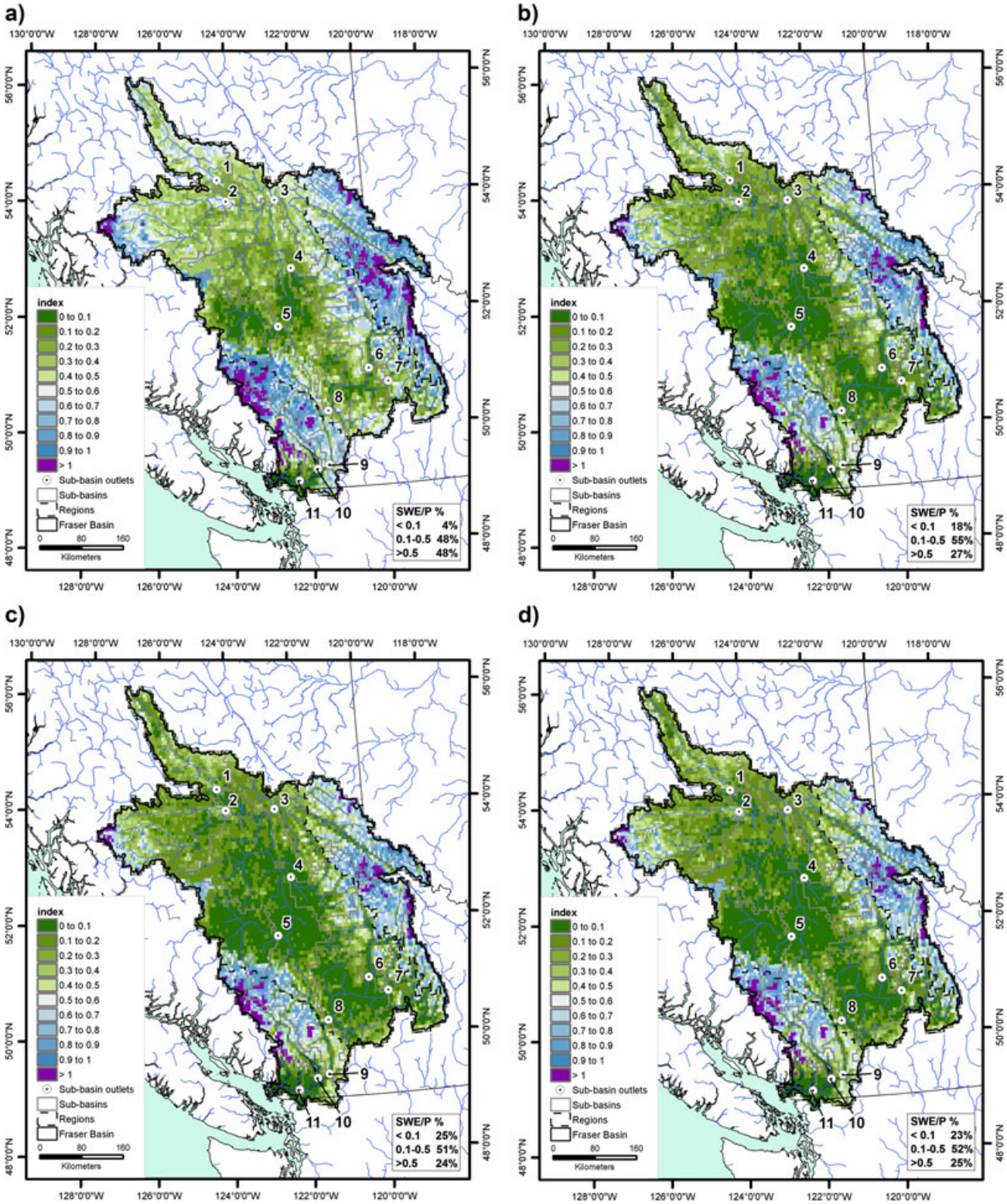

Figure 7. Ratios of April 1st snow water equivalent to October-March precipitation (SWE/P). Illustrated ratios are for: a) 1970s; and median of the 2050s ensembles of the b) B1; c) A1B and d) A2 emissions scenarios.

(not shown) lead to general decrease in autumn runoff. The spatial pattern of future runoff changes also show variability, with more pronounced change in the eastern and coastal mountains compared to the central plateau region.

Future discharge and runoff responses for the sub-basins and regions of the FRB are shown in Figures 10 and 11, respectively. Future projections for all three scenarios show noticeable changes from the baseline period with generally greater change (increase or decrease) for the A1B and A2 scenarios and smaller change for the B1 scenario. Such differences amongst the three scenarios also correspond to the SWE (Table VI), and SWE/P (Figure 7) changes, illustrating the effects

DOI: 10.1002/hyp

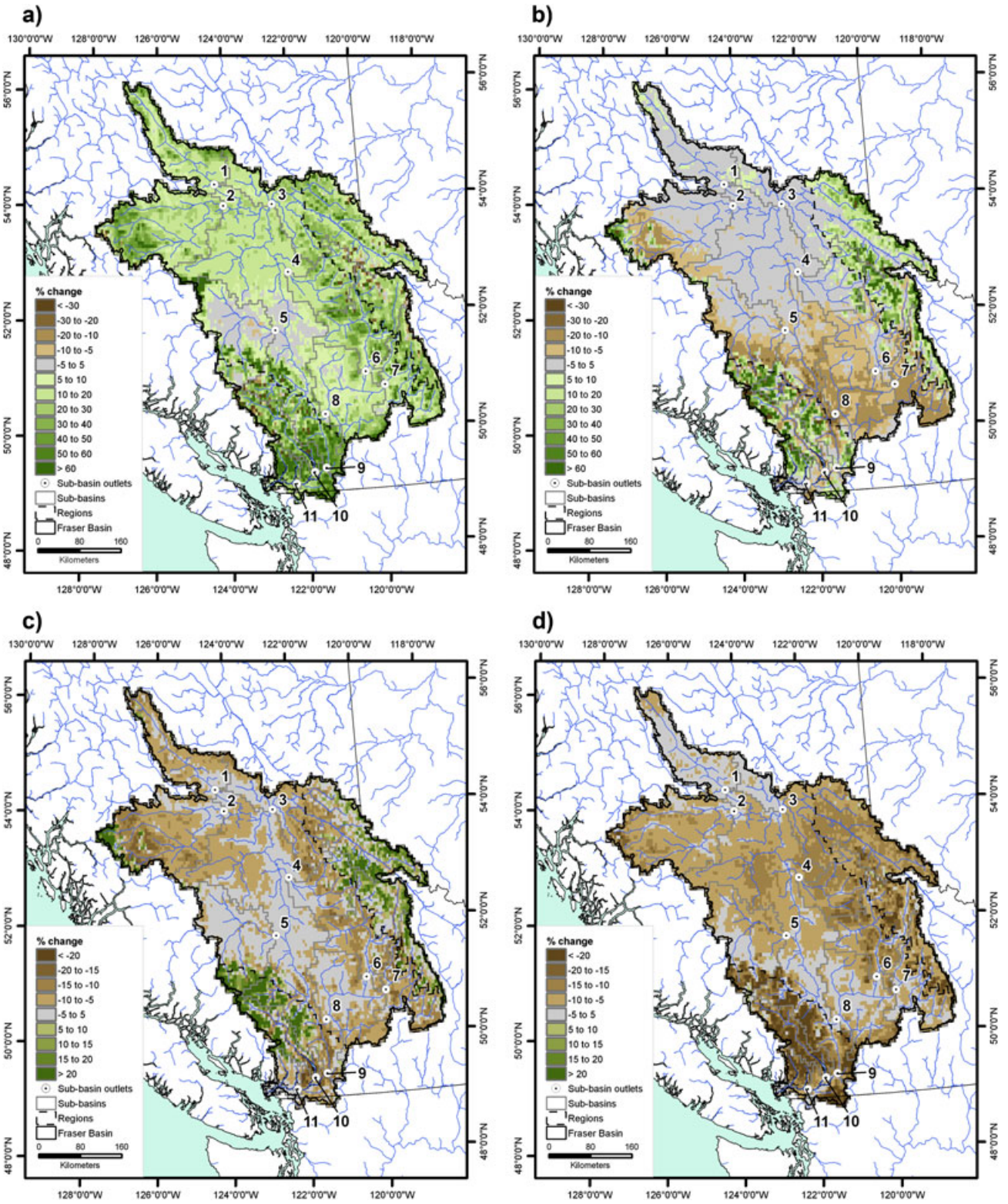

Figure 8. Median A1B evapotranspiration anomalies [%] (2050s *versus* 1970s) for a) spring, b) summer; and median A1B soil moisture anomalies [%] (2050s *versus* 1970s) c) June 1st, d) September 1st.

of temperature and precipitation changes for the three scenarios (Table V) on the snowmelt and runoff regimes. Overall, in comparison to the 1970s, 2050s winter-spring (December-May) monthly mean discharge (routed flow at the catchment outlet) is generally projected to increase for all three scenarios and 11 sub-basins of the FRB. Higher winter-spring precipitation, regime transition (transition from snow-dominant and hybrid regimes to hybrid, and rain-dominant regimes, respectively) and the earlier decline of seasonal snow storage (compared to baseline period) lead to such changes. The changes also affect the autumn-winter discharge patterns in the basin. Specifically, in contrast to the baseline period, which is characterized by steady

DOI: 10.1002/hyp

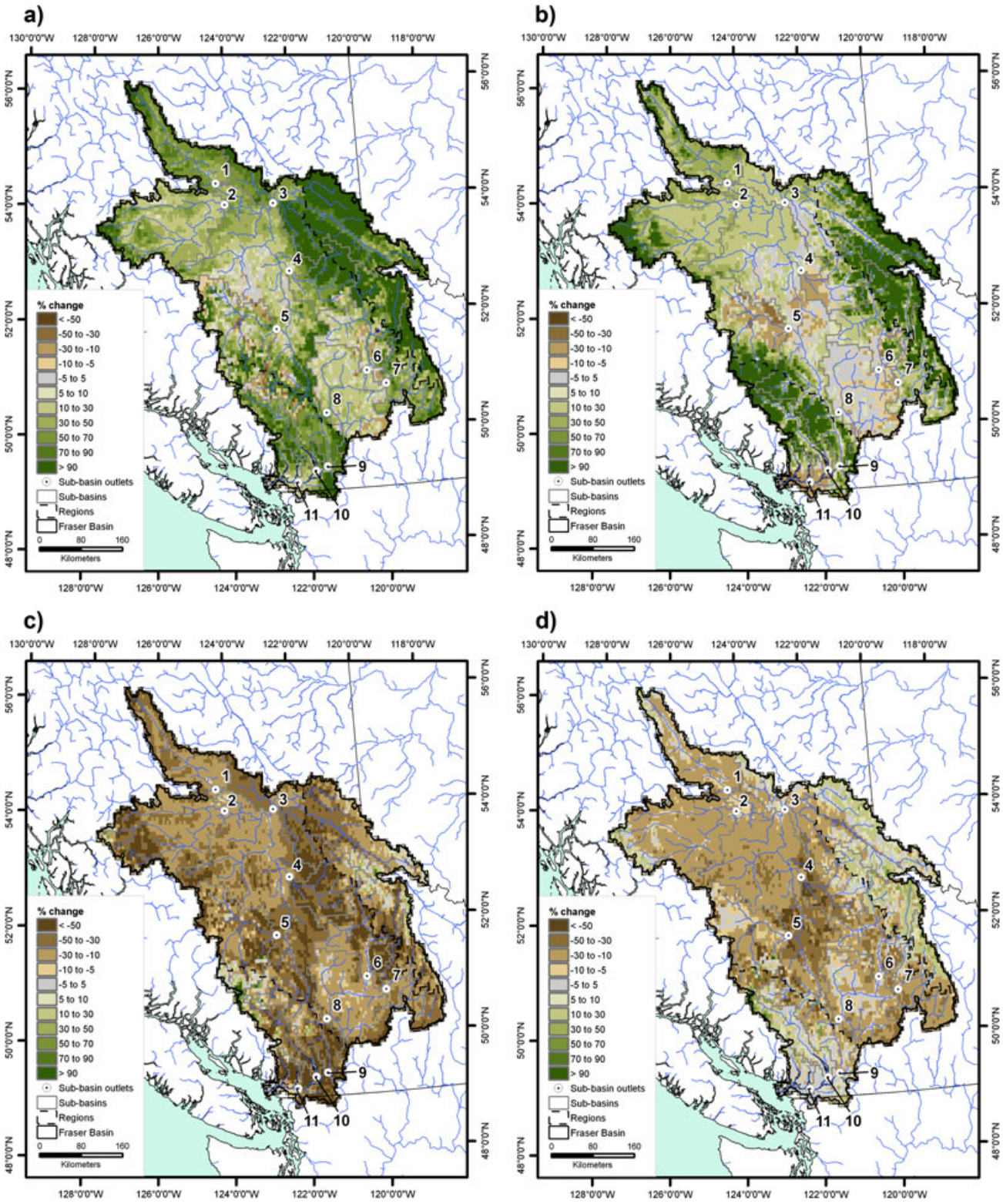

Figure 9. Median A1B runoff anomalies [%] (2050s *versus* 1970s) for the FRB for a) winter, b) spring, c) summer and d) autumn.

decline in discharge from autumn to winter, a less pronounced decline (e.g. Fraser-Shelly and Quesnel sub-basins) or an increase (e.g. Stuart and Nechako sub-basins) is simulated for the future period. Spring discharge also shows a distinctive change from 1970s to 2050s with an increase in monthly discharge for most GCMs and emission scenarios. These are followed by lower summer discharge, mostly due to lower precipitation, and soil moisture and snowpack depletion in the previous spring months.

Although the responses amongst the sub-basins are similar, some differences in runoff responses (mean grid cell flow response for a region) from the three regions can be seen. Specifically, while 2050s winter runoff for the eastern and coastal mountains is lower than autumn runoff, winter runoff is higher than autumn runoff in the

DOI: 10.1002/hyp

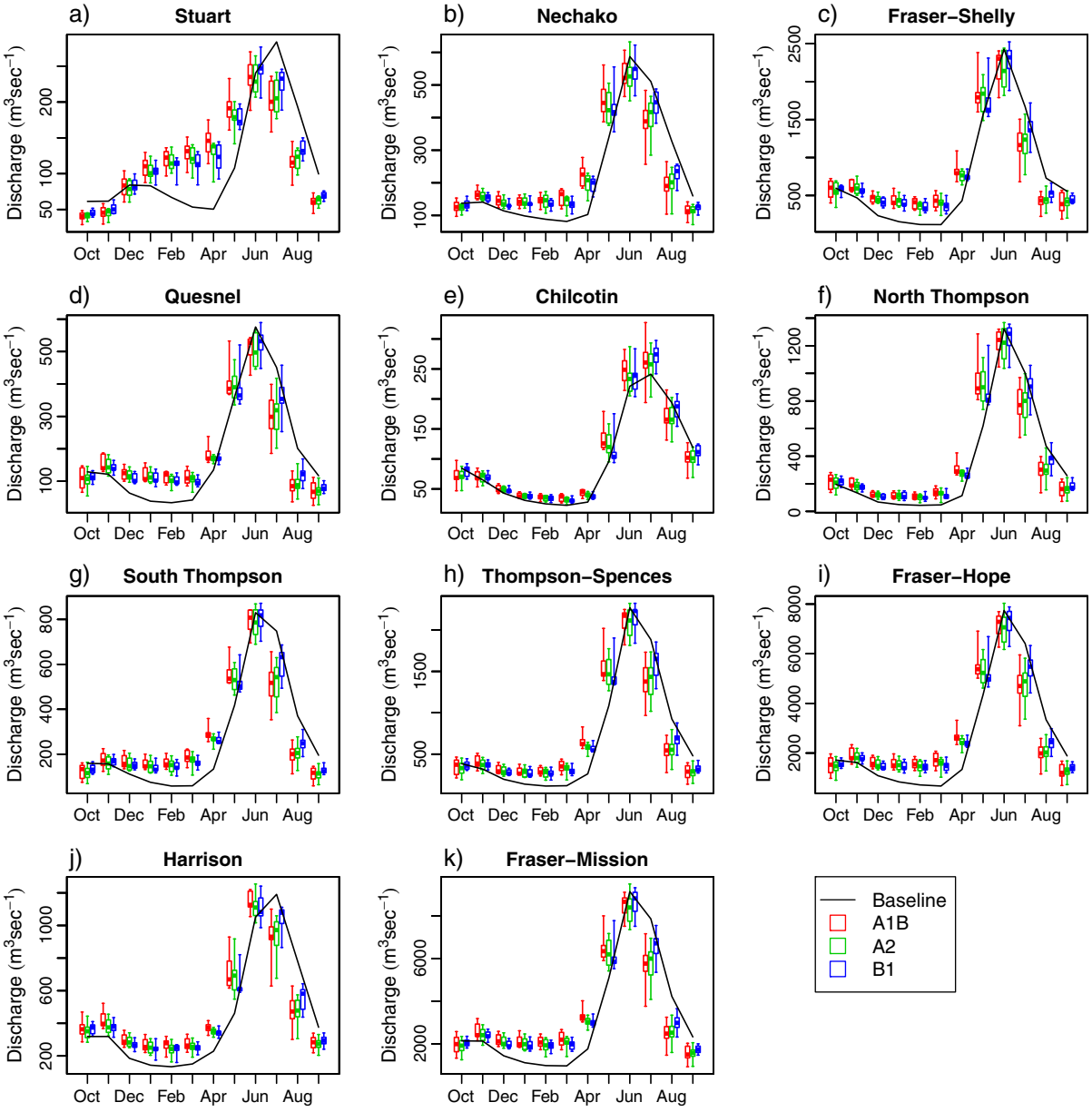

Figure 10. Baseline (1970s) and future (2050s) discharge [m^3/s] for the sub-basins of the FRB. Each box plot illustrates the median and inter-quartile range, and the whiskers upper and lower limits of the 30-year means of GCM ensembles.

interior plateau region. Such differences in the interior plateau region correspond to the shift from hybrid to rain-dominant regime in some parts of the region (Figure 7). Another noticeable difference is in the timing of the runoff peak, while the future runoff peaks for the eastern and coastal mountains region occur in June, the peak runoff for the interior plateau occurs in May, indicating an earlier depletion of seasonal snow storage. Such differences are also related to the variable soil moisture changes in the basin as depicted by the June 1st values (Figure 8c), which show increased soil moisture in the coastal and eastern mountains and decreased soil moisture in the central plateau. Differences in the future response in the three regions are also illustrated by changes in the seasonal runoff ratios (expressed as the ratio of December-May to June-November runoff), with the values increasing from 0.24 to 0.47–0.69 (the ranges correspond to the median values of three emission scenarios), 0.48 to 0.82–1.08 and 0.82 to 1.34–1.57 for the eastern mountains, coastal mountains and central plateau, respectively. Such differences indicate that while the eastern mountains will remain summer-autumn runoff dominant, the central plateau will transition to a winter-spring dominant regime.

The effect of temperature-driven shifts in the discharge is also evident in the timing of the peak discharge (Figure 12). An earlier onset of discharge is simulated for all sub-basins of the FRB, which can be explained as the effect of earlier snowmelt driven by higher temperature. Such shifts amongst the 11 sub-basins vary between 2 days and 25 days (median values) for B1, 10 days and 39 days for A1B and 10 days and 43 days for A2 scenarios. The greater shifts for the A1B and A2 scenarios compared to B1 are due to higher temperature increases for the scenarios. Also related to the change in the snow storage is the annual

DOI: 10.1002/hyp

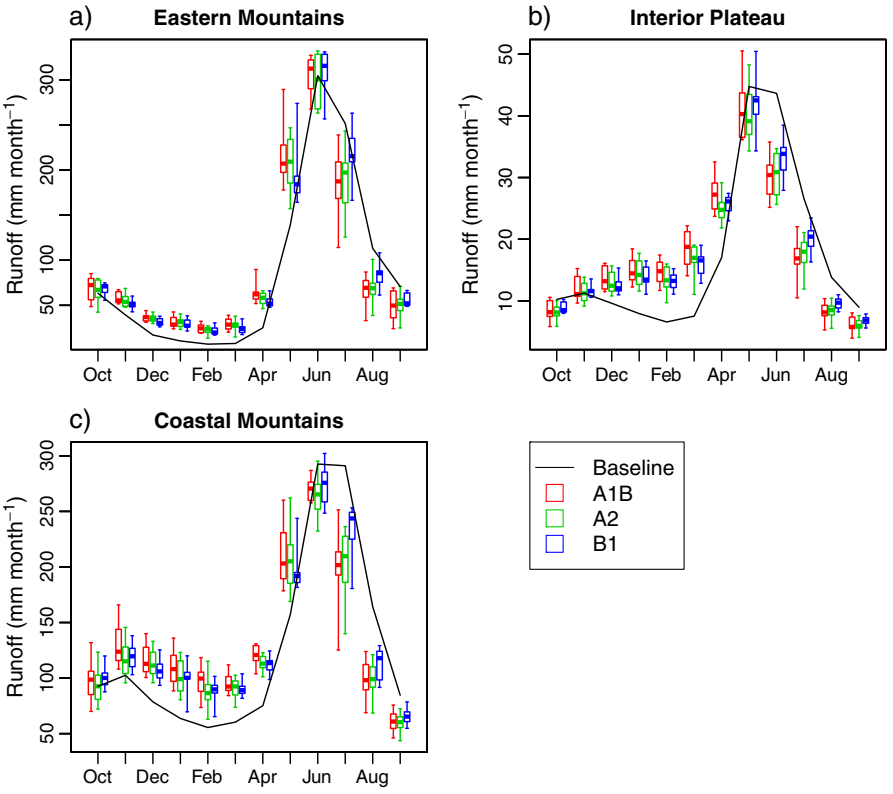

Figure 11. Baseline (1970s) and future (2050s) runoff [mm/month] for the three regions of the FRB. Each box plot illustrates the median and inter-quartile range, and the whiskers upper and lower limits of the 30-year means of GCM ensembles.

peak discharge. The GCM ensemble medians of the 30-year mean annual peak discharge depict decreases for most sub-basins and scenarios (Figure 13). Decreased peak discharge is projected despite increased winter and spring precipitation. Such changes illustrate that the temperature-driven change in snow storage affects both the timing and magnitude of discharge peaks. As illustrated by (Hamlet and Lettenmaier, 2007), such

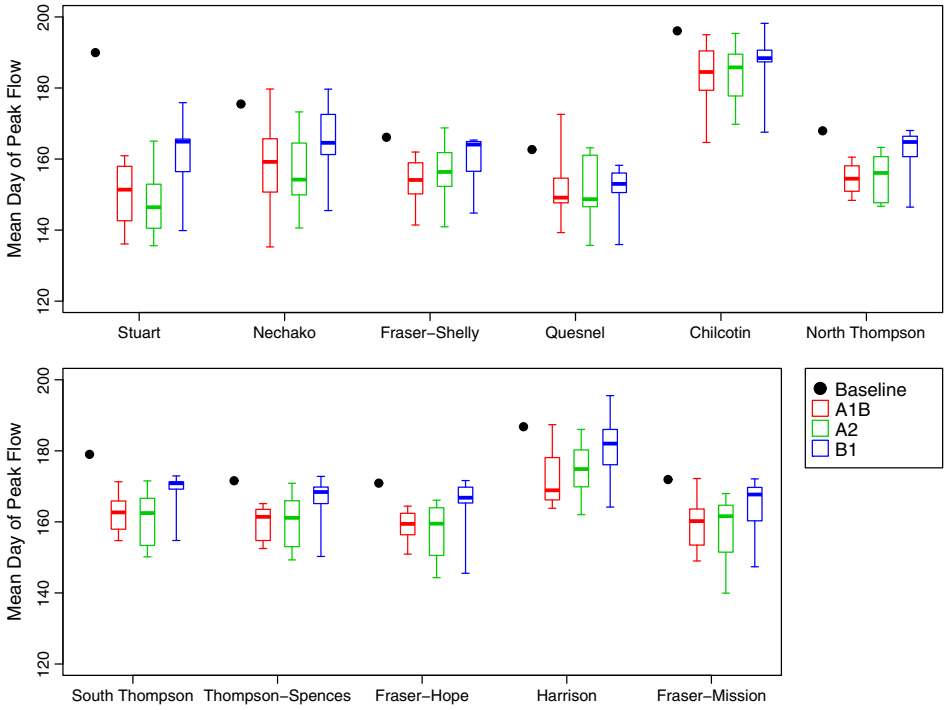

Figure 12. Julian day of occurrence of annual peak discharge for the baseline (1970s) and future (2050s) periods for the sub-basins of the FRB. Each box plot illustrates the median and inter-quartile range, and the whiskers upper and lower limits of the 30-year means of GCM ensembles.

DOI: 10.1002/hyp

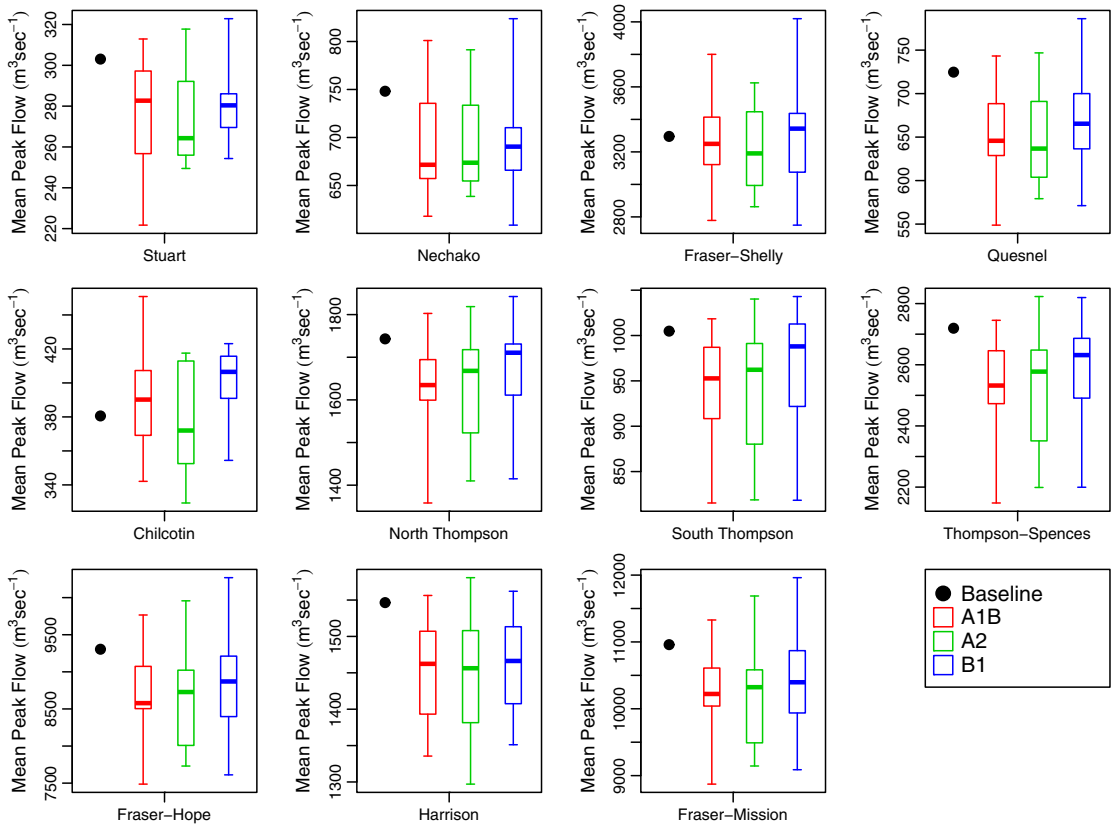

Figure 13. 30-year mean annual peak discharge [m^3/s] for the baseline (1970s) and future (2050s) periods for the sub-basins of the FRB. Each box plot illustrates the median and inter-quartile range, and the whiskers upper and lower limits of the 30-year means of GCM ensembles.

changes could also have implications on the sensitivity of flood risk.

The box and whisker plots of discharge and runoff projections also depict wide ranges indicating large uncertainty in the mean projection from the GCM ensembles (Figures 10 and 11). For instance, for the Fraser-Mission station, the largest range in the projected future discharge can be seen in the month of July (B1 ~ 3400 m^3/s; A2 ~ 2900 m^3/s and A1B ~ 2200 m^3/s), which is more than 25% of the mean baseline discharge (7900 m^3/s). Although the ranges are smaller for the winter-early spring months, such as March (B1 ~ 950 m^3/s; A2 ~ 940 m^3/s and A1B ~ 630 m^3/s), the ranges are more than 65% of the mean baseline discharge (970 m^3/s). The range of 30-year mean annual peak discharge and day of occurrence of the peak annual discharge also vary considerably. For instance, for the Fraser-Mission station, the ranges of peak discharge are more than 2000 m^3/s (Figure 13) for three scenarios, while, date of peak flow could vary by 20 days (Figure 12). The wide range of future projections obtained from a suite of GCMs and their respective emissions scenarios again reinforces the need to use an ensemble GCM approach to sample a range of possible future changes.

However, despite such differences in the ranges, the VIC model simulated discharge (for the sub-basins) and runoff (for the regions) show consistent increases in the median annual values obtained from the GCM ensembles (Table VI). Amongst the three scenarios, greater annual discharge increases are projected for the B1 emission scenario. The differences can be explained by higher precipitation increases (Table V) and lower summer flow decreases for the B1 scenario. The discharge increases for the sub-basins also generally correspond to the precipitation increases. For example, the relatively larger discharge increases in the northern sub-basins of Stuart and Fraser-Shelly correspond to relatively larger precipitation increases for these sub-basins. Median annual runoff increases in the eastern and central mountain regions, while the central plateau shows smaller increases (B1 scenario) or decreases (A1B and A2 scenarios). Given that precipitation in the eastern and coastal mountains is higher than the central plateau, increased precipitation amount is also higher in these regions, which likely causes higher runoff increases. However, since most sub-basins are located within multiple regions, such differences are not evident in the sub-basin discharge response.

SUMMARY AND CONCLUSIONS

The ensemble GCM-driven VIC hydrologic model simulation for the FRB revealed that a warmer climate is likely to bring considerable hydrologic changes. Snow accumulation and melt is one of the key processes likely to be affected, with April 1st SWE projected to decline for most of the basins, which is in agreement with projected changes in the PNW (e.g. Chang and Jung, 2010; Elsner *et al.*, 2010). The declines are lower for the mountainous

DOI: 10.1002/hyp

sub-basins and regions as compared to the central plateau region, indicating variable depletion of snow storage across the basin. The analysis of regime characteristics of the basin using the SWE to precipitation ratio suggests successive shifts from snow-dominant to hybrid, and hybrid to rain-dominant regime in some areas of the basin.

The results of this study also indicate variability in the seasonal runoff response. While summer runoff is generally projected to decrease, winter and spring runoff are projected to increase. Summer changes are mainly due to decreased precipitation and earlier snowmelt. The winter and spring runoff increases are mainly due to precipitation increases and early depletion of the snowpack (compared to the baseline period) in the basin. The effect of the change in the snowpack storage is also evident in the simulated spring discharge peak, which is projected to occur earlier throughout the sub-basins of the FRB. Such changes are consistent with the observed past trend in the basin (e.g. Morrison *et al*., 2002) and elsewhere in the region (e.g. Mote *et al*., 2005; Stewart, 2009). In addition, the GCM ensemble medians of the 30-year mean annual peak discharge depict decreases for most sub-basins and scenarios.

This study also showed that future hydrologic response can vary regionally. For instance, the modelled scenarios depict variable changes in the runoff regimes, with shifts from snow-dominant to hybrid regime mainly occurring in the eastern and coastal mountains and hybrid to rain-dominant regimes mainly occurring in the central plateau region. The related winter-spring to summer-autumn runoff ratios also revealed variable future changes, with runoff for the eastern mountains projected to remain summer-autumn dominant and the central plateau projected to change to winter-spring dominant. Consequently, more pronounced winter runoff increases are projected in the central plateau region. Furthermore, mean annual runoff is projected to increase in the wetter parts of the basin (eastern and coastal mountains), while runoff is projected to increase slightly or decrease in the drier parts of the basin (central plateau).

The future precipitation and runoff changes for the 2050s obtained from different driving GCMs vary considerably. Specifically, for the 23 simulations (7 GCMs x 3 scenarios + 1 GCMs x 2 scenarios), precipitation change varies between −5% and 17% for the entire area upstream of the Fraser-Mission hydrometric station, and the discharge change ranged between −10% and 19%. Such changes in discharge increase/decrease (±10%) for the FRB are also projected by the previous study by Kerkhoven and Gan (2011) using seven GCM-driven runs. However, the variability of the future discharge changes is larger in this study, especially when considering the three regions. Specifically, for the eastern mountains, central plateau and the coastal mountains regions, mean annual precipitation changes vary between −2% and 20%, −6% and 15%, and −7% and 18%, while the mean annual runoff changes vary between −8% and 20%, −15% and 17%, and −7% and 20%, respectively.

The results of this hydrologic impact study are affected by uncertainties associated with the GCMs, downscaling method and hydrologic model. The wide range of future projections obtained from a suite of GCMs and their respective emissions scenarios depict considerable uncertainties associated with the GCMs. Such range reinforces the need to use an ensemble GCM approach and provides a range of possible future changes for different plausible forcings. Downscaling uncertainty such as using monthly GCM outputs and daily resampling, and hydrologic model uncertainties in representing various elements of a hydrograph also add to uncertainties of the projected future changes. Specifically, uncertainties in the VIC modelling include model input, parameter model structure uncertainties such as the lack of accounting of glaciers. About 1.5% of the FRB is glaciated and the loss of glaciers could significantly impact responses from some of the sub-basins, such as, Harrison (15% glacier coverage), Chilcotin (4.6%), North Thompson (4.3%), and Fraser-Shelly (2.5%). As illustrated by Huss (2011) in a study of glacier storage in macroscale drainage basins in Europe, glacier loss could lead to a reduction in summer flow in these sub-basins, larger than that depicted by the current study. The mountain pine beetle infestation could also add to uncertainties in the simulated hydrologic response. Previous analysis on mountain pine beetle outbreak in the FRB (Schnorbus *et al*. 2010) indicates that forest infestation tends to increase peak flow magnitude, with the relative change in magnitude increasing with increasing forest disturbance severity. The study also suggests higher peak flow sensitivity to the cumulative effects of beetle-kill and salvaging harvesting than to beetle-kill alone. Therefore, future studies should consider the combined impacts of forest disturbance and climate change. In addition, methods to account for model uncertainties (e.g. glaciers), and analysis of changes to hydro-ecological flow indicators such as high and low flow matrices should be a focus for future research.

The differences in the future hydrologic responses across the basin also support the need for a spatial and temporal evaluation of future hydrologic change. Such an approach is especially relevant for large river basin like the FRB, where physiographic and climatic characteristics vary considerably. Moreover, the spatial and temporal evaluation of future responses will allow for consideration of adaption strategies more suited for local conditions. The projected future changes in the FRB could have important implications for regional water resources management, such as hydropower generation, fisheries and recreation. The change in the snow storage and runoff timing, especially the reduction of summer runoff, could have implications for water storage. The reduction in the summer runoff could especially affect water availability in the dry central plateau region. Therefore, the results of this study provide stakeholders with hydro-climatic projections that can be used for local-scale adaptation in this important water resource system in the province.

DOI: 10.1002/hyp

ACKNOWLEDGEMENTS

The authors are thankful to Francis Zwiers (PCIC) for providing useful comments to the manuscript. Katrina Bennett formally at PCIC (now at the University of Alaska, Fairbanks) is gratefully acknowledged for preparation of vegetation, soil and snowband data and generation of the meteorological gridded forcings. The authors also wish to acknowledge PCIC's Geographic Information Systems Analyst, Hailey Eckstrand, for data processing and mapping. The authors thank the reviewers for their comments toward an improved version of the manuscript.

REFERENCES

Adam JC, Clark EA, Lettenmaier DP, Wood EF. 2006. Correction of Global Precipitation Products for Orographic Effects. *Journal of Climate* **19**(1): 15–38.

Adam J, Hamlet A, Lettenmaier D. 2009. Implications of global climate change for snowmelt hydrology in the twenty-first century. *Hydrological Processes* **23**(7): 962–972.

Barnett TP, Adam JC, Lettenmaier DP. 2005. Potential impacts of a warming climate on water availability in snow-dominated regions. *Nature* **438**: 303–309.

Barnett TP, Pierce DW, Hidalgo HG, Bonfils C, Santer BD, Das T, Bala G, Wood AW, Nozawa T, Mirin AA, Cayan DR, Dettinger MD. 2008. Human-induced changes in the hydrology of the western United States. *Science* **319**: 1080–1083.

Bennett KE, Werner AT, Schnorbus M. 2012. Uncertainties in hydrologic and climate change impact analyses in headwater basins of British Columbia. *Journal of Climate* (in press). DOI: 10.1175/JCLI–D–11–00417.1

Beven K, Freer J. 2001. Equifinality, data assimilation, and uncertainty estimation in mechanistic modelling of complex environmental systems using the GLUE methodology. *Journal of Hydrology* **249**(1–4): 11–29.

Blöschl G, Montanari A. 2010. Climate change impacts—throwing the dice? *Hydrological Processes* **24**(3): 374–381.

Bürger G, Murdock TQ, Werner AT, Sobie SR, Cannon AJ. 2012. Downscaling extremes – an intercomparison of multiple statistical methods for present climate. *Journal of Climate*, doi: 10.1175/JCLID–11–00408.1, in press.

Chang HJ, Jung IW. 2010. Spatial and temporal changes in runoff caused by climate change in a complex large river basin in Oregon. *Journal of Hydrology* **388**: 186–207.

Cherkauer KA, Sinha T. 2010. Hydrologic impacts of projected future climate change in the Lake Michigan region. *Journal of Great Lakes Research* **36**: 33–50.

Christensen NS, Lettenmaier DP. 2007. A multimodel ensemble approach to assessment of climate change impacts on the hydrology and water resources of the Colorado River Basin. *Hydrology and Earth System Sciences* **11**: 1417–1434.

Christensen NS, Wood AW, Voisin N, Lettenmaier DP, Palmer RN. 2004. The effects of climate change on the hydrology and water resources of the Colorado River basin. *Climatic Change* **62**(1–3): 337–363.

Collins W, Bitz C, Blackmon M, Bonan G, Bretherton C, Carton J, Chang P, Doney S, Hack J, Henderson T, Kiehl J, Large W, McKenna D, Santer B, Smith R. 2006. The Community Climate System Model version 3 (CCSM3). *Journal of Climate* **19**(11): 2122–2143.

Collins M, Tett S, Cooper C. 2001. The internal climate variability of HadCM3, a version of the Hadley Centre coupled model without flux adjustments. *Climate Dynamics* **17**(1): 61–81.

Cunderlik JM, Ouarda T. 2009. Trends in the timing and magnitude of floods in Canada. *Journal of Hydrology* **375**: 471–480.

Cuo L, Beyene TK, Voisin N, Su FG, Lettenmaier DP, Alberti M, Richey JE. 2011. Effects of mid-twenty-first century climate and land cover change on the hydrology of the Puget Sound basin, Washington. *Hydrological Processes* **25**(11): 1729–1753.

Daly C, Neilson RP, Phillips DL. 1994. A Statistical-Topographic Model for Mapping Climatological Precipitation over Mountainous Terrain. *Journal of Applied Meteorology* **33**(2): 140–158.

Delworth T, Broccoli A, Rosati A, Stouffer R, Balaji V, Beesley J, Cooke W, Dixon K, Dunne J, Dunne K, Durachta J, Findell K, Ginoux P, Gnanadesikan A, Gordon C, Griffies S, Gudgel R, Harrison M, Held I, Hemler R, Horowitz L, Klein S, Knutson T, Kushner P, Langenhorst A, Lee H, Lin S, Lu J, Malyshev S, Milly P, Ramaswamy V, Russell J, Schwarzkopf M, Shevliakova E, Sirutis J, Spelman M, Stern W, Winton M, Wittenberg A, Wyman B, Zeng F, Zhang R. 2006. GFDL's CM2 global coupled climate models. Part I: Formulation and simulation characteristics. *Journal of Climate* **19**(5): 643–674.

Demaria EM, Nijssen B, Wagener T. 2007. Monte Carlo sensitivity analysis of land surface parameters using the Variable Infiltration Capacity model. *Journal of Geophysical Research-Atmospheres* **112**: D11113.

Elsner MM, Cuo L, Voisin N, Deems JS, Hamlet AF, Vano JA, Mickelson KEB, Lee SY, Lettenmaier DP. 2010. Implications of 21st century climate change for the hydrology of Washington State. *Climatic Change* **102**(1–2): 225–260.

Fleming SW, Whitfield PH, Moore RD, Quilty EJ. 2007. Regime-dependent streamflow sensitivities to Pacific climate modes cross the Georgia–Puget transboundary ecoregion. *Hydrological Processes* **21**(24): 3264–3287.

Foreman MGG, Lee DK, Morrison J, Macdonald S, Barnes D, Williams IV. 2001. Simulations and retrospective analyses of fraser watershed flows and temperatures. *Atmosphere-Ocean* **39**(2): 89–105.

Gao H, Tang Q, Shi X, Zhu C, Bohn TJ, Su F, Sheffield J, Pan M, Lettenmaier DP, Wood EF. in review. Water Budget Record from Variable Infiltration Capacity (VIC) Model. In Algorithm Theoretical Basis Document for Terrestrial Water Cycle Data Records.

Global Soil Data Task. 2000. Global Soil Data Products CD-ROM (IGBP-DIS). CD-ROM. International Geosphere-Biosphere Programme, Data and Information System, Potsdam, Germany. Available from Oak Ridge National Laboratory Distributed Active Archive Center, Oak Ridge, Tennessee, U.S.A.

Gonzalez P, Neilson PR, Lenihan JM, Drapek RJ. 2010. Global patterns in the vulnerability of ecosystems to vegetation shifts due to climate change. *Global Ecology and Biogeography* **19**(6): 755–768.

Hamlet AF, Lettenmaier DP. 2007. Effects of 20th century warming and climate variability on flood risk in the western U.S. *Water Resources Research* **43**: 17.

Hamlet AF, Mote PW, Clark MP, Lettenmaier DP. 2005. Effects of temperature and precipitation variability on snowpack trends in the western United States. *Journal of Climate* **18**: 4545–4561.

Hidalgo HG, Das T, Dettinger MD, Cayan DR, Pierce DW, Barnett TP, Bala G, Mirin A, Wood AW, Bonfils C, Santer BD, Nozawa T. 2009. Detection and Attribution of Streamflow Timing Changes to Climate Change in the Western United States. *Journal of Climate* **22**(13): 3838–3855.

Huntington TG. 2006. Evidence for intensification of the global water cycle: Review and synthesis. *Journal of Hydrology* **319**: 83–95.

Huss M. 2011. Present and future contribution of glacier storage change to runoff from macroscale drainage basins in Europe. *Water Resources Research* **47**. doi:10.1029/2010WR010299.

Jarvis A, Reuter HI, Nelson A, Guevara E. 2008. Hole-filled seamless SRTM data V4 583 International Centre for Tropical Agriculture (CIAT), http://srtm.csi.cgiar.org (accessed June 2011).

Jung IW, Chang HJ. 2011. Assessment of future runoff trends under multiple climate change scenarios in the Willamette River Basin, Oregon, USA. *Hydrological Processes* **25**(2): 258–277.

K-1 Model Developers. 2004. K-1 coupled GCM (MIROC) description. H. Hasumi and S Emori (Eds.). K-1 Technical Report 1, Center for Climate System Research, University of Tokyo; National Institute for Environmental Studies (NIES), Frontier Research Center for Global Change (FRCGC).http://www.ccsr.u–tokyo.ac.jp/kyosei/hasumi/MIR-OC/tech–repo.pdf (accessed March 2011).

Kay AL, Davies HN, Bell VA, Jones RG. 2008. Comparison of uncertainty sources for climate change impacts: flood frequency in England. *Climatic Change* **92**(1–2): 41–63.

Kerkhoven E, Gan TY. 2011. Differences and sensitivities in potential hydrologic impact of climate change to regional-scale Athabasca and Fraser River basins of the leeward and windward sides of the Canadian Rocky Mountains respectively. *Climatic Change* **106**(4): 583–607.

Kimmins JP. 2005. Forest ecology. In: Forestry Handbook for British Columbia, Watts, SB, Tolland, L (eds). The Forestry Undergraduate Society, University of British Columbia: Vancouver, BC; 434–471.

Kundzewicz ZW, Mata LJ, Arnell NW, Döll P, Kabat P, Jiménez B, Miller KA, Oki T, Sen Z, Shiklomanov IA. 2007. Freshwater resources and their management. M.L. Parry, O.F. Canziani, J.P. Palutikof, P.J. van der Linden and C.E. Hanson, (Eds.). Climate Change 2007: Impacts, Adaptation and Vulnerability. Contribution of Working Group II to the Fourth Assessment Report of the Intergovernmental Panel on Climate Change, Cambridge University Press, Cambridge, UK: 173–210.

Kurz WA, Dymond CC, Stinson G, Rampley GJ, Neilson ET, Carroll AL, Ebata T, Safranyik L. 2008. Mountain pine beetle and forest carbon feedback to climate change. *Nature* **452**: 987–990.

Laval BE, Morrison J, Potts DJ, Carmack EC, Vagle S, James C, McLaughlin FA, Foreman M. 2008. Wind-driven Summertime Upwelling in a Fjord-type Lake and its Impact on Downstream River Conditions: Quesnel Lake and River, British Columbia, Canada. *Journal of Great Lakes Research* **34**(1): 189–203.

Liang X, Lettenmaier DP, Wood EF, Burges SJ. 1994. A simple hydrologically based model of land-surface water and energy fluxes for general-circulation models. *Journal of Geophysical Research-Atmospheres* **99**(D7): 14415–14428.

Liang X, Wood EF, Lettenmaier DP. 1996. Surface soil moisture parameterization of the VIC-2L model: Evaluation and modification. *Global and Planetary Change* **13**(1–4): 195–206.

Lohmann D, Raschke E, Nijssen B, Lettenmaier D. 1998. Regional scale hydrology: I. Formulation of the VIC-2 L model coupled to a routing model. *Hydrological Sciences Journal-journal Des Sciences Hydrologiques* **43**(1): 131–141.

Marlon JR, Bartlein PJ, Walsh MK, Harrison SP, Brown KJ, Edwards ME, Higuera PE, Power MJ, Anderson RS, Briles C, Brunelle A, Carcaillet C, Daniels M, Hu FS, Lavoie M, Long C, Minckley T, Richard PJH, Scott AC, Shafer DS, Tinner W, Umbanhowar CE, Whitlock C. 2009. Wildfire response to abrupt climate change in North America. *Proceedings of the National Academy of Science of the USA* **106**(8): 2519–2524.

Martin G, Ringer M, Pope V, Jones A, Dearden C, Hinton T. 2006. The physical properties of the atmosphere in the new Hadley Centre Global Environmental Model (HadGEM1). *Part I: Model description and global climatology. Journal of Climate* **19**(7): 1274–1301.

Maurer EP, Hidalgo HG. 2008. Utility of daily vs. monthly large-scale climate data: An intercomparison of two statistical downscaling methods. *Hydrology and Earth System Sciences* **12**(2): 551–563.

Maurer EP, Wood AW, Adam JC, Lettenmaier DP, Nijssen B. 2002. A long-term hydrologically based dataset of land surface fluxes and states for the conterminous United States. *Journal of Climate* **15**: 3237–3251.

Merritt WS, Alila Y, Barton M, Taylor B, Cohen S, Neilsen D. 2006. Hydrologic response to scenarios of climate change in sub watersheds of the Okanagan basin, British Columbia. *Journal of Hydrology* **326**: 79–108.

Moore RD. 1991. Hydrology and Water Supply in the Fraser River Basin. In Water in Sustainable Development: Exploring Our Common Future in the Fraser River Basin, AHJ Dorcey, JR Griggs (eds). Wastewater Research Centre, The University of British Columbia: Vancouver, British Columbia, Canada; 21–40.

Moore RD, Wondzell SM. 2005. Physical hydrology and the effects of forest harvesting in the Pacific Northwest: A review. *Journal of the American Water Resources Association* **41**(4): 763–784.

Moore RD, Trubilowicz JW, Buttle JM. 2012. Prediction of streamflow regime and annual runoff for ungauged basins using a distributed monthly water balance model. *Journal of the American Water Resources Association* **1–11**, DOI: 10.1111/j.1752–1688.2011.00595.x.

Morrison J, Quick MC, Foreman MGG. 2002. Climate change in the Fraser River watershed: flow and temperature projections. *Journal of Hydrology* **263**: 230–244.

Mote PW, Hamlet AF, Clark MP, Lettenmaier DP. 2005. Declining mountain snowpack in western north America. *Bulletin of the American Meteorological Society* **86**(1): 39-+.

Mundie JH, Bell-Irving R. 1986. Predictability of the Consequences of the Kemano Hydroelectric Proposal for Natural Salmon Populations. *Canadian Water Resources Journal* **11**(1): 14–25.

Najafi MR, Moradkhani H, Jung IW. 2011. Assessing the uncertainties of hydrologic model selection in climate change impact studies. *Hydrological Processes* **25**(18): 2814–2826.

Neilsen D, Duke G, Taylor B, Byrne J, Kienzle S, Van der Gulik T. 2010. Development and Verification of Daily Gridded Climate Surfaces in the Okanagan Basin of British Columbia. *Canadian Water Resources Journal* **35**(21): 131–154.

Pelletier P. 1990. A review of techniques used by Canada and other northern countries for measurement and computation of streamflow under ice conditions. *Nordic Hydrology* **21**(4–5): 317–340.

Prudhomme C, Davies H. 2008a. Assessing uncertainties in climate change impact analyses on the river flow regimes in the UK. Part 1: baseline climate. *Climatic Change* **93**: 177–195.

Prudhomme C, Davies H. 2008b. Assessing uncertainties in climate change impact analyses on the river flow regimes in the UK. Part 2: future climate. *Climatic Change* **93**: 197–222.

Rauscher SA, Pal JS, Diffenbaugh NS, Benedetti MM. 2008. Future changes in snowmelt-driven runoff timing over the western US. *Geophysical Research Letters* **35**: L16703.

Rice SP, Church M, Wooldridge CL, Hickin EJ. 2009. Morphology and evolution of bars in a wandering gravel-bed river; lower Fraser river, British Columbia, Canada. *Sedimentology* **56**(3): 709–736.

Rodenhuis D, Bennett KE, Werner AT, Murdock TQ, Bronaugh D. 2009: Climate overview 2007: Hydro-climatology and future climate impacts in British Columbia. Pacific Climate Impacts Consortium, University of Victoria: Victoria, BC; 132.

Roeckner E, Brokopf R, Esch M, Giorgetta M, Hagemann S, Kornblueh L, Manzini E, Schlese U, Schulzweida U. 2006. Sensitivity of simulated climate to horizontal and vertical resolution in the ECHAM5 atmosphere model. *Journal of Climate* **19**(16): 3771–3791.

Rotstayn LD, Collier MA, Dix MR, Feng Y, Gordon HB, O'Farrell SP, Smith IN, Syktus J. 2010. Improved simulation of Australian climate and ENSO-related rainfall variability in a global climate model with an interactive aerosol treatment. *International Journal of Climatology* **30**: 1067–1088.

Schnorbus M, Bennett K, Werner A. 2010. Quantifying the water resources impacts of the mountain pine beetle and associated salvage harvest operations across a range of watershed scales: Hydrologic modelling of the Fraser River Basin, MBPI Project 7.29, Natural Resources Canada, Canadian Forest Service, Pacific Forestry Centre, Information Report BC-X-423, 64 p.

Schnorbus MA, Bennett KE, Werner AT, Berland AJ. 2011. Hydrologic Impacts of Climate Change in the Peace, Campbell and Columbia Watersheds, British Columbia, Canada. Pacific Climate Impacts Consortium, University of Victoria: Victoria, BC; 157.

Scinocca JF, McFarlane NA, Lazare M, Li J, Plummer D. 2008. Technical Note: The CCCma third generation AGCM and its extension into the middle atmosphere. *Atmospheric Chemistry and Physics* **8**: 7055–7074.

Shrestha RR, Rode M. 2008. Multi-objective calibration and fuzzy preference selection of a distributed hydrological model. *Environmental Modelling & Software* **23**: 1384–1395.

Stahl K, Moore RD, Floyer JA, Asplin MG, McKendry IG. 2006. Comparison of approaches for spatial interpolation of daily air temperature in a large region with complex topography and highly variable station density. *Agricultural and Forest Meteorology* **139**(3–4): 224–236.

Stewart IT. 2009. Changes in snowpack and snowmelt runoff for key mountain regions. *Hydrological Processes* **23**(1): 78–94.

Stewart IT, Cayan DR, Dettinger MD. 2005. Changes toward earlier streamflow timing across western North America. *Journal of Climate* **18** (5): 1136–1155.

Thorne R, Woo M. 2011. Streamflow response to climatic variability in a complex mountainous environment: Fraser River Basin, British Columbia, Canada. *Hydrological Processes* **25**(19): 3076–3085.

Todini I. 1996. The ARNO rainfall-runoff model. *Journal of Hydrology* **175**(1–4): 339–382.

Vano JA, Voisin N, Cuo L, Hamlet AF, Elsner MM, Palmer RN, Polebitski A, Lettenmaier DP. 2010. Climate change impacts on water management in the Puget Sound region, Washington State, USA. *Climatic Change* **102**(1–2): 261–286.

Wade NL, Martin J, Whitfield PH. 2001. Hydrologic and Climatic Zonation of Georgia Basin, British Columbia. *Canadian Water Resources Journal* **26**(1): 43–70.

Wang T, Hamann A, Spittlehouse DL, Murdock TQ. 2012. ClimateWNA—High-Resolution Spatial Climate Data for Western North America. *Journal of Applied Meteorology and Climatology* **51**(1): 16–29.

Werner AT. 2011. BCSD Downscaled Transient Climate Projections for Eight Select GCMs over British Columbia, Canada. Pacific Climate Impacts Consortium, University of Victoria: Victoria, BC; 63.

Whitfield PH, Cannon AJ, Reynolds CJ. 2002. Modelling Streamflow in Present and Future Climates: Examples from the Georgia Basin, British Columbia. *Canadian Water Resources Journal* **27**(4): 427–456.

Whitfield PH, Wang JY, Cannon AJ. 2003. Modelling Future Streamflow Extremes — Floods and Low Flows in Georgia Basin, British Columbia. *Canadian Water Resources Journal* **28**(4): 633–656.

Wood A, Leung L, Sridhar V, Lettenmaier D. 2004. Hydrologic implications of dynamical and statistical approaches to downscaling climate model outputs. *Climatic Change* **62**(1–3): 189–216.

Wulder M, Dechka J, Gillis M, Luther J, Hall R, Beaudoin A. 2003. Operational mapping of the land cover of the forested area of Canada with Landsat data: EOSD land cover program. *The Forestry Chronicle* **79**(6): 1075–1083.

Yapo PO, Gupta HV, Sorooshian S. 1998. Multi-objective global optimization for hydrologic models. *Journal of Hydrology* **204**(1–4): 83–97.